

# Nuclear Liquid Drop Model with the Surface-Curvature Terms: New Perspectives for the Hyperdeformation Studies\*

K. Pomorski<sup>1,2</sup> and J. Dudek<sup>1</sup>

<sup>1</sup>*Institut de Recherches Subatomiques, IN<sub>2</sub>P<sub>3</sub>-CNRS/Université Louis Pasteur  
F-67037 Strasbourg Cedex 2, France*

<sup>2</sup>*Katedra Fizyki Teoretycznej, Uniwersytet Marii Curie-Skłodowskiej,  
PL-20031 Lublin, Poland*

## Abstract

Nuclear liquid drop model is revisited and an explicit introduction of the surface-curvature terms is presented. The corresponding parameters of the extended classical energy formula are adjusted to the contemporarily known nuclear binding energies and fission barrier heights. Using 2766 binding energies of nuclei with  $Z \geq 8$  and  $N \geq 8$  it is shown that the performance of the new approach is improved by a factor of about 6, compared to the previously published liquid drop model results, in terms of both the masses (new r.m.s. deviation  $< \delta M > = 0.698$  MeV) and the fission barriers (new r.m.s. deviation of the fission barriers of isotopes with  $Z > 70$  is  $< \delta V_B > = 0.88$  MeV).

The role of the curvature terms and their effects on the description of the experimental quantities are discussed in detail; for comparison the parameters of the more 'traditional' approaches are re-fitted taking into account the nuclear masses known today and the performances of several variants of the model are compared. The isospin dependence in the new description of the barriers is in a good agreement with the extended Thomas-Fermi approach; it also demonstrates a good qualitative agreement with the fission life-time systematics tested on the long chain of Fermium isotopes known experimentally.

The new approach offers also a very high stability in terms of the extrapolation from the narrower range of nuclides to a more extended one - a property of particular interest for the contemporary exotic beam projects: the

---

\*This work has been partly supported by the Polish Committee for Scientific Research under Contract No. 2P03B 115 19 and by the Program No. 99-95 of Scientific Exchange between the IN<sub>2</sub>P<sub>3</sub>, France, and Polish Nuclear Research Institutions.

corresponding properties are illustrated and discussed.

PACS numbers: 24.75.+i, 25.85.-w, 25.60.Pj, 25.70-z

## I. INTRODUCTION

It is more than sixty years by now since the first successful application of the charged liquid-drop model to describe the nuclear binding energies [1,2]. Brilliant extensions of the Bethe-Weizsäcker nuclear drop concept by Meitner and Frisch [3] and by Bohr and Wheeler [4] have been obtained in 1939 and used to explain the nuclear fission phenomenon. Since then many papers have been devoted to the nuclear liquid drop model formalism and its improvements. Various new terms in the corresponding energy expressions have been proposed but the basic concept of the charged liquid drop which could deform and fission remained valid. It is worth reminding at this point that already in 1953 Hill and Wheeler concluded on the basis of the Fermi gas model, Ref. [5], that a curvature dependent term proportional to  $A^{1/3}$  should exist in the liquid drop energy functional. The curvature term was later studied in Ref. [6] where its magnitude was adjusted to the known at that time experimental fission barrier heights.

The macroscopic model description of the nuclear masses and, more generally, the nuclear deformation energies using Strutinsky-type approaches, plays a very important role in the large scale nuclear energy calculations that allow programming new important experiments such as e.g. on super- or on still hypothetical hyper-deformations at high angular momenta. The existence of the hyperdeformed nuclear configurations has been predicted on the basis of the realistic large scale calculations - the same calculations that predicted the existence of several islands of the super-deformed nuclei. While the presence of the latter has been confirmed experimentally on several dozens of cases, there is so far no single convincing experimental evidence for the former. On the one hand, problems related to the increased *instrumental* sensitivity, when looking for manifestations of the hyperdeformed configurations had to be expected. On the other hand it is clearly of importance to look for sources of possibly systematic and perhaps not so well controlled effects in the theoretical large scale calculations performed so far, and one may hope that by combining the two different types of efforts some new steps forward will be possible.

A possible mechanism to discuss that has not been taken into account in the large scale calculations in question is related to the interpretation and more generally to the mathematical representation of the classical nuclear surface energy. Deformation-dependent classical energy expressions can be seen as functions of two groups of variables that describe, respectively, the nucleus itself,  $(Z, N)$ , and its shape represented by an ensemble of the deformation parameters, here abbreviated to  $\{\alpha\}$ . Typically, the surface energy is written as a product  $E_s(Z, N; \{\alpha\}) = f(Z, N)g(\{\alpha\})$ , where the first factor is usually parametrized by introducing a few adjustable constants e.g.  $f(N, Z) = p_0 + p_1(N - Z)/(N + Z)$  or any other expression of this type that is found performant;  $p_1$  and  $p_2$  are adjustable constants, whose number does not need to be limited to 2. As it has been discussed already by other authors, in a more careful approach the nuclear surface energy can be seen as contributed by *two* different but related geometrical elements: the numerical value of surface area and the surface's average curvature (cf. Eqs. (2.7) - (2.9) below and the corresponding text). Such an argument implies a different form of the surface energy expression:  $E_s(Z, N; \{\alpha\}) = f_a(Z, N)g_a(\{\alpha\}) + f_c(Z, N)g_c(\{\alpha\})$ , where indices *a* and *c* refer to area and curvature, respectively, and where the deformation dependencies of  $g_a$  and  $g_c$  are different; moreover, in the spirit of the classical nuclear energy models the corresponding factors  $f_a(Z, N)$  and

$f_c(Z, N)$  are to be adjusted separately. By re-fitting all the adjustable parameters of the classical energy expression to the experimental masses of over two thousands of nuclei as well as on the fission barriers we are going to look for the most performant parameterization to be used in conjunction with the Strutinsky type formalism. In such an approach all the terms including the surface energy term will be represented 'as optimally as possible'<sup>1</sup> in a global fit'.

Let us emphasize that interpretations of classical models that simulate quantum properties of nuclei must not be associated too directly to the notions of non-existing objects such as *classical forces* supposed to act on the nucleons e.g. in the vicinity of the nuclear surface. Strictly speaking, classical interpretations involving such forces that are related either to the *surface tension* or *surface curvature* do not make much sense for the strongly interacting Fermi systems. This implies in particular that in the present context the corrective curvature term does not need to have any definite sign and the optimal effect can be obtained by taking, say, a larger area-contribution accompanied by smaller curvature-contribution, or, to the contrary, with a slightly smaller area-contribution accompanied instead by a larger curvature-term. In fact the surface energy contributions in the more traditional approaches and in the present approach are close in terms of their numerical values but the present approach that distinguishes between the *surface-area* contribution and the *surface-curvature* contribution turns out to approximate the whole ensemble of the known nuclear masses and barriers in a more flexible way. In particular the new r.m.s. deviation will be shown to be  $\langle \delta M \rangle = 0.698$  MeV compared to  $\langle \delta M \rangle = 0.732$  MeV within the traditional approach, and the new fission barrier r.m.s. deviation for nuclei with  $Z > 70$ ,  $\langle \delta V_B \rangle = 0.88$  MeV, compared to  $\langle \delta V_B \rangle = 5.58$  MeV.

Several studies performed in the past, of the contributions coming from the surface curvature to the total energy, aimed at estimating its value using a more elementary (microscopic) ideas about the nuclear interactions, both for the finite nuclei and for the semi-infinite nuclear matter media. Some of the corresponding papers are mentioned below; much more details about that evolution can be found in the articles quoted therein. In particular, using the energy density formalism of Ref. [7] combined with the macroscopic formulation of the curvature energy expressions of Myers and Świątecki, [8], Stocker, Ref. [9], pointed to the compatibility of the curvature energy estimates coming from the two approaches. Grammaticos, Ref. [10], using the Skyrme type functional, but limiting himself to the terms of the order of  $\hbar^2$ , was able to obtain what could be considered as a reasonable estimate for the curvature energy, stressing however that the results are sensitive to the details of the energy functional and pointing to the necessity of including higher order terms. This has been done for instance in Ref. [11], where also a comparison of the results of various calculations and estimates known at the time of publication can be found. However, the main results obtained

---

<sup>1</sup> We expect that the *area* contribution  $\sim f_a \cdot g_a$  should be a dominating factor since the traditional liquid drop model without explicit use of the curvature energy term performed quite well already; the surface-curvature term is expected to be smaller and to play a role of a correction. We will demonstrate that such a fit is possible and corresponds to a significant improvement of performance of the liquid drop model formula.

by the authors, were compatible with the earlier theoretical predictions. A more distinct link between microscopic and macroscopic models was proposed in Ref. [12], where various terms of the droplet model were derived from the Skyrme interaction, in the framework of the extended Thomas-Fermi (ETF) model. The problem of self-consistency, when approaching the issue of the curvature energy, has been addressed in [13]; no major influence of this aspect of the formalism on the final result has been found. Relativistic mean-field theory within semi-classical approach has been applied, Ref. [14], to the semi-infinite nuclear matter concluding that the relativistic and the more traditional methods give in essence compatible results. Extension to the relativistic but quantum approaches has been studied in Ref. [15] with the conclusion that also within the relativistic approaches the semi-classical and fully quantum approaches give consistent, comparable results. Similar physical goals but within relativistic Hartree approximation have been approached in [16] and sensitivity of the final result to the related physical quantities such as the (in)compressibility coefficient and nucleonic effective-mass has been discussed. Also, a detailed, more recent analysis of the problem of the surface and curvature energies using Skyrme type interactions but aiming principally at the astrophysical applications can be found in Ref. [17], see also references therein.

Let us stress that the above mentioned developments addressed first of all the problem of an existence of relationships between the nuclear curvature energy (terms in the total nuclear energy expression proportional to  $A^{1/3}$ ) and a microscopic representation of the nuclear forces, together with the role of such elements and mechanisms as the order of expansion in the extended Thomas-Fermi model, type of the Skyrme forces, comparison between the semi-classical and the quantum calculation results, as well as the possible influence of the relativistic effects. All these studies point coherently to the result that the first order curvature coefficient should be of the order of, typically, 5 to 15 MeV. At the same time most of the more phenomenological approaches, based directly on the *global fits* to the experimental data pointed to the value very close to zero. In fact, in several studies the corresponding term was often altogether neglected, and the discrepancy mentioned turned into a kind of a 'curvature anomaly' problem. This contradiction (energy contribution that should exist according to most of the physical/theoretical arguments *vs.* fits within the multi-parametric macroscopic model that give almost vanishing contributions) can possibly be indicative of a peculiarity contained in the macroscopic energy dependence on its parameters, that makes it impossible to extract the non-zero values of the curvature terms from the data on the masses the way these extractions were attempted: below, possible alternative fitting procedures will be discussed and their results compared.

There is also another group of studies that were focused more specifically on the calculations of the nuclear masses and/or the deformation dependence in the classical energy expressions that, supplemented with the Strutinsky and pairing quantum energy terms could be used for studying such problems as nuclear fission, super- and hyper-deformation and more generally the shape coexistence phenomena. A few years ago, a realistic Thomas-Fermi (TF) model has been developed by Myers and Świątecki [18], that describes masses of known nuclei with high accuracy (the main ingredients of this model are shortly recalled in Appendix A). The corresponding r.m.s. deviation between the experimental [19] and theoretical binding energies for 1654 isotopes amounts to 0.655 MeV only. In the last decade more than one thousand masses of new isotopes have been measured and in the new edition of the Strasbourg Chart of Nuclides [20] one can find 2766 binding energies of the isotopes

with the proton and neutron numbers larger than  $Z=N=8$  (cf. Fig. 1). The r.m.s. deviation of the TF estimates for these 2766 masses is 0.758 MeV and shows a high numerical precision of the model as well as a good accuracy of the shell and pairing energies obtained in Ref. [21] that the TF model adopts. Fission barrier heights evaluated on the basis of the Thomas-Fermi model [18,22] are also in a rather good agreement with the experimental data.

A significant progress in the self-consistent methods has taken place in the recent years as well. For instance, the Hartree-Fock mass formula of Tondeur *et al.*, Ref. [23], that employs the effective *MSk7* Skyrme interaction was able to reproduce the 1888 experimental binding energies with the r.m.s. deviation of 0.738 MeV. This r.m.s. deviation increases to only 0.828 MeV when one makes the comparison with 2766 experimental masses taken from table [20].

At present the self-consistent and the macroscopic-microscopic methods play both their important roles in the nuclear structure calculations. While the latter are very well suited for e.g. the 'automatic' large scale calculations of the total nuclear energy surfaces, fission barriers, high spin properties, shape-isomerism studies and/or numerous excited particle-hole configurations, the former are extremely useful in the detailed theoretical description of the nuclear states whose *global features* are already known. The simplicity of the macroscopic nuclear drop formalism together with the clear physical meaning of its parameters add definitely to its attractiveness; it is easy to apply and thus frequently used in particular in estimating the fusion and fission cross sections in heavy ions reactions.

A particular motivation for the present work is to obtain a new set of parameters of the liquid drop model adjusted to the up-to-date experimental masses *and* fission barriers, while taking a particular care of the surface-curvature aspects of the model. This is of special importance when studying the exotic nuclear shapes such as the nuclear hyper-deformation and/or the nuclear path to fission (e.g. the bi-modal or more complex fission phenomena). The nuclear surface-curvature aspects were so far not analyzed very much in detail, at least recently. As precise as possible a liquid drop model description combined with the powerful shell energy description within the mean-field theories offers invaluable services.

A starting point of our analysis is the well known, 'traditional', liquid drop nuclear mass expression of Myers and Świątecki (MS-LD) [26]. This expression was quite successful in reproducing the nuclear masses but it is known that in the light nuclei it overestimates the fission barrier heights by up to about 10 MeV [27]; the MS-LD barriers are also higher than those evaluated by Sierk [28] within the Yukawa-folded-interaction macroscopic model.

It is of an obvious importance to assure the stability of the final result with respect to the cut off in terms of the number of multipoles used. All the fission-barrier heights presented in this paper were obtained by minimizing with respect to the deformation parameters  $\beta_\lambda$  of even  $\lambda$  up to  $\lambda_{max} = 14$ . In order to test the stability of our minimization procedure with respect to this cut off, we have performed additional test-minimizations using the Trentalange-Koonin-Sierk (TKS) family of shapes defined in Ref. [29]. The multipole and the TKS parameterizations clearly differ, yet the resulting fission barriers almost coincide when number of the  $\beta_\lambda$  parameters is sufficiently large. On the one hand, to obtain the same accuracy one needs typically twice as many multipoles as TKS deformation parameters. On the other hand we found out that the  $\beta_\lambda$  parameterization is more stable than the TKS one when performing the numerical minimization of the potential energy surfaces (PES). Going beyond  $\lambda_{max} = 14$  does not change the final fission barrier results in the studied cases by

more than a couple of hundreds of keV for the highest barriers calculated here, i.e. in the  $A \sim 80$  mass range, while for the heavier nuclei the modifications are of the order of dozens of keV, an accuracy totally sufficient in the present context.

Direct calculations show that the Yukawa-folded-interaction model, which gives rather reasonable estimates of the fission barriers, is too soft in directions perpendicular to the fission path especially at the large nuclear elongation. It will be of great interest trying to combine (and we will demonstrate that it is possible) an improved description of the fission barriers together with a better description of the above mentioned stiffness behavior within one single approach.

The paper is organized as follows: The actual version of the liquid drop model used is described in Section II. In Section III we specify the way in which the parameters were determined and we present the best sets of parameters for various variants of the LD models.

Our results concerning the fission barriers are presented in Section IV. The paper is summarized in Section V, where also an outlook of the planned applications of the obtained results is presented.

## II. LIQUID DROP MODEL AND MICROSCOPIC ENERGY FUNCTIONAL

We are going to recapitulate briefly the main ideas of the leptodermous expansion [30] of the energy-density functional in order to introduce the presentation of the role of the nuclear surface curvature-terms.

### A. General Considerations

The integral of the energy functional, the latter obtained e.g. by a self-consistent calculation, can be expanded into a power series of  $A^{1/3}$  if one assumes that the energy-density function and the density of nucleons are diffused in the region of the nuclear surface (cf. e.g. Ref. [12]). Let us denote the nuclear radius by  $R$ , the nuclear surface thickness by  $a$ , and assume that  $a/R \ll 1$  as well as that mass number  $A$  is so large that  $A^{-1/3} \ll 1$ .

Let  $\hat{H}$  denote the many-body Hamiltonian and  $\Psi$  the corresponding many-body ground state wave function of a nucleus. The one-body density of the nuclear matter in the nucleus can be expressed as

$$\rho = A \int \int \dots \int \Psi^* \Psi d\tau_2 \dots d\tau_A, \quad (2.1)$$

and the corresponding energy density as

$$\eta = \int \int \dots \int \Psi^* \hat{H} \Psi d\tau_2 \dots d\tau_A. \quad (2.2)$$

The total energy of the nucleus is equal to the volume integral of the energy density

$$E = \int_V \eta d^3\mathbf{r}; \quad (2.3)$$

it can be decomposed into the sum of the volume term and of another term that contains an integral over the nuclear surface  $\Sigma$ :

$$E = \int_V (\eta + b_{\text{vol}} \rho - b_{\text{vol}} \rho) d^3 \mathbf{r} = b_{\text{vol}} \int_V \rho d^3 \mathbf{r} + \int_V (\eta - b_{\text{vol}} \rho) d^3 \mathbf{r} \quad (2.4a)$$

$$= b_{\text{vol}} A + \int_{\Sigma} d\sigma \int_0^{\infty} (\eta - b_{\text{vol}} \rho) dr_{\perp}. \quad (2.4b)$$

The difference under the last integral in Eq. (2.4b) can be expected to partially cancel out in the nuclear interior, the most significant contribution coming from the surface region. The remaining expression can be interpreted as the integral over the nuclear surface  $\Sigma$  of the surface-tension  $\gamma$ , the latter formally defined by

$$\gamma \equiv \int_0^{\infty} (\eta - b_{\text{vol}} \rho) dr_{\perp}. \quad (2.5)$$

Let us introduce the principal radii  $R_1$  and  $R_2$  that are associated locally to any point on the nuclear surface  $\Sigma$ . In geometry, the local properties of surfaces are conveniently expressed in terms of the first order curvature  $\kappa$  and the second order (Gauss) curvature  $\Gamma$  defined through

$$\kappa = \frac{1}{R_1} + \frac{1}{R_2} \quad \text{and} \quad \Gamma = \frac{1}{R_1 \cdot R_2}, \quad (2.6)$$

respectively. These *local* quantities can be shown to underly important and interesting in the present context *global* properties. Indeed, it is easy to see that in geometrical terms, the volume  $\mathcal{V}$  enclosed by a given surface  $\mathcal{S}$ , the surface itself and the implied average curvature  $\mathcal{L}$  are directly correlated through the equation of the surface since one may write

$$\mathcal{V} = \frac{1}{3} \int_{\mathcal{S}} d\vec{\sigma} \cdot \vec{r}, \quad (2.7a)$$

$$\mathcal{S} = \int_{\mathcal{S}} d\sigma, \quad (2.7b)$$

$$\mathcal{L} = \int_{\mathcal{S}} d\sigma \left( \frac{1}{R_1} + \frac{1}{R_2} \right). \quad (2.7c)$$

An instructive next step can be obtained by considering a family of some special surfaces, the one-parameter Steiner sheets  $\{\mathcal{S}(s)\}$ , having the property of being universally equidistant. More precisely, for any two values of parameter  $s$ , say,  $s_1$  and  $s_2$ , the corresponding normal distances are constant and equal  $|s_2 - s_1|$ . For such surfaces it can be shown that

$$\mathcal{L}(s) = \frac{d\mathcal{S}}{ds} = \frac{d^2\mathcal{V}}{ds^2} \quad (2.8)$$

with the consequence, as remarked in Ref. [6], that for the Taylor expansions, e.g. at  $s = 0$ , one finds

$$\mathcal{V}(s) = \mathcal{V}_0 + \mathcal{S}_0 s + \frac{1}{2} \mathcal{L}_0 s^2 + \dots \quad (2.9a)$$

$$\mathcal{S}(s) = \mathcal{S}_0 + \mathcal{L}_0 s + \dots, \quad (2.9b)$$

where  $\mathcal{V}_0$ ,  $\mathcal{S}_0$  and  $\mathcal{L}_0$  are constants, equal to the values of the functions in Eq. (2.8) at  $s = 0$ . Relations of an analogous mathematical structure are used more generally in the LD



approximations and also below in this article. In the form (2.9) they show that the average curvature indeed characterizes the volume and the surface within Taylor expansion of the second and first order, respectively, and that this quantity is indeed a natural geometric feature to introduce in the related physical considerations<sup>2</sup>. The above relations are suggestive of yet another important possibility related to the question of the sign of the curvature term that has been for some time also a discussed issue. The surface effect represented by the Taylor expansion of  $\mathcal{S}(s)$  in Eq. (2.9b), is a sum of two terms, and as it stands suggests that both  $\mathcal{S}_0$  and  $\mathcal{L}_0$  are uniquely defined constants. In the applications, however, the procedure followed is different: the expressions that mathematically resemble the above relation(s) are still used but the parameters are *fitted* using *Steiner-like* surfaces rather than using Steiner's theorem. Consequently, whenever  $\mathcal{S}_0$  is found slightly larger, the corresponding  $\mathcal{L}_0$  will provide a compensation, including a possibility that  $\mathcal{L}_0 < 0$ . We believe that in the present context of the Taylor-expansion type of analysis it would have been inappropriate to associate a definite sign of such a contribution as 'more physical than the other' - in contrast - the sign of the whole surface contribution could be attributed physical sense.

It can be shown that for the surface of sufficient regularity the *average* Gauss curvature defined in analogy to the average first order curvature through the corresponding surface integral satisfies

$$\int_S d\sigma \left( \frac{1}{R_1 \cdot R_2} \right) = 4\pi, \quad (2.10)$$

independently of the actual shape; this feature will have interesting consequences for the reproduction of the nuclear masses (see below).

One can expect that the local surface tension depends on the diffusivity of the surface region (represented by the diffusivity parameter  $a$ ) as well as on the two curvatures. For dimensionality reasons it will be convenient to parameterize this dependence as

$$\gamma = \gamma(a\kappa, a^2\Gamma). \quad (2.11)$$

The above function can be decomposed into a Taylor series around the argument values  $a\kappa = 0$  and  $a^2\Gamma = 0$  and we obtain

$$\gamma(a\kappa, a^2\Gamma) = \gamma^{(0)} + \gamma'_\kappa \kappa a + \frac{1}{2}\gamma''_{\kappa\kappa} \kappa^2 a^2 + \gamma'_\Gamma \Gamma a^2 + \dots, \quad (2.12)$$

where  $\gamma^{(0)}$ ,  $\gamma'_\kappa$ ,  $\gamma''_{\kappa\kappa}$  and  $\gamma'_\Gamma$  are constants. Inserting the latter expression into the surface integral in Eq. (2.4b) we may transform the surface contribution to the energy of the system to the following form:

$$\int_V (\eta - b_{\text{vol}} \rho) d^3\mathbf{r} = \gamma^{(0)} \int_\Sigma d\sigma + \gamma'_\kappa a \int_\Sigma \kappa d\sigma + \frac{1}{2}\gamma''_{\kappa\kappa} a^2 \int_\Sigma \kappa^2 d\sigma + \gamma'_\Gamma a^2 \int_\Sigma \Gamma d\sigma + \dots \quad (2.13)$$

---

<sup>2</sup>The surfaces used in the macroscopic description of nuclei are in general not strict examples of Steiner sheets. Yet, in many cases the regular surfaces used are expected to behave in a very similar manner; the very fact that the expansions used in physics resemble those in Eq. (2.9) and work well in physical applications strongly suggests that this is in fact the case.

Since for the nuclear surfaces we have  $\int_{\Sigma} d\sigma \sim A^{2/3}$  while  $\kappa \sim A^{-1/3}$  and  $\Gamma \sim A^{-2/3}$  it follows that the terms appearing in the last relation can be alternatively parametrized as

$$\gamma^{(0)} \int_{\Sigma} d\sigma \rightarrow b_{\text{surf}} A^{2/3} B_{\text{surf}}, \quad (2.14a)$$

$$\gamma'_{\kappa} a \int_{\Sigma} \kappa d\sigma \rightarrow b_{\text{cur}} A^{1/3} B_{\text{cur}}, \quad (2.14b)$$

$$\frac{1}{2} \gamma''_{\kappa\kappa} a^2 \int_{\Sigma} \kappa^2 d\sigma + \gamma'_{\Gamma} a^2 \int_{\Sigma} \Gamma d\sigma \rightarrow b_{\text{curG}} A^0, \quad (2.14c)$$

where we have inserted an explicit dependence of various terms on powers of  $A^{1/3}$  as well as the corresponding proportionality coefficients. The nuclear deformation-dependent functions  $B_{\text{surf}}$  and  $B_{\text{cur}}$  in relations (2.14a) and (2.14b) are defined, respectively, as ratios of the surface and the mean-curvature, calculated at a given deformation, to the corresponding values at the spherical shapes. The Gaussian curvature energy (the last term in relation (2.14c)) is deformation independent but may introduce an important dependence in terms of isospin when fitting the related liquid drop parameters to the experimental masses; the first term in the correspondence relation (2.14c) is small and its dependence on deformation, which we shall neglect later, can be found in Ref. [12], cf. Eq. (5.21) in the above reference.

The nuclear part of the total energy of a nucleus can thus be given by the following final expression

$$E = b_{\text{vol}} A + b_{\text{surf}} A^{2/3} + b_{\text{cur}} A^{1/3} + b_{\text{curG}} A^0 + \dots; \quad (2.15)$$

the Coulomb part will be introduced later.

## B. Particular Case: Spherical Nuclei

It is instructive to study the properties of expression (2.15) in the case of spherical nuclei. In this case the second integral in (2.4b) can be rewritten as follows:

$$E = b_{\text{vol}} A + \int_V (\eta - b_{\text{vol}} \rho) d^3 \mathbf{r} \quad (2.16a)$$

$$= b_{\text{vol}} A + \int_{\Sigma} R^2 d\Omega \int_0^{\infty} (\eta - b_{\text{vol}} \rho) \frac{r^2}{R^2} dr, \quad (2.16b)$$

where  $R$  (usually represented as  $R = r_0 A^{1/3}$ ) is the radius of the spherical surface. Making use of the identity:

$$\frac{r^2}{R^2} = 1 + \frac{2}{R}(r - R) + \frac{1}{R^2}(r - R)^2, \quad (2.17)$$

one can rewrite the remaining surface-related integral and transform the energy expression as follows

$$E = b_{\text{vol}} A \quad (2.18a)$$

$$+ \int_{\Sigma} R^2 d\Omega \int_0^{\infty} (\eta - b_{\text{vol}} \rho) dr \quad (2.18b)$$

$$+ \int_{\Sigma} 2R d\Omega \int_0^{\infty} (\eta - b_{\text{vol}} \rho) (r - R) dr \quad (2.18c)$$

$$+ \int_{\Sigma} d\Omega \int_0^{\infty} (\eta - b_{\text{vol}} \rho) (r - R)^2 dr. \quad (2.18d)$$

Above, expressions (2.18b), (2.18c) and (2.18d), contain terms proportional to  $R^2$ ,  $R^1$  and  $R^0$ , respectively, thus at the same time, proportional to  $A^{2/3}$ ,  $A^{1/3}$  and  $A^0$ . In the present context they should be interpreted as representing the surface, curvature and Gauss-curvature contributions, correspondingly. The nuclear part of the total energy of a spherical nucleus can thus be written down as

$$E = b_{\text{vol}}A + \underbrace{4\pi R^2 \cdot \mathcal{I}_0}_{b_{\text{surf}}A^{2/3}} + \underbrace{8\pi R \cdot (\mathcal{I}_1 - \mathcal{I}_0 R)}_{b_{\text{cur}}A^{1/3}} + \underbrace{4\pi \cdot (\mathcal{I}_2 - 2R\mathcal{I}_1 + R^2\mathcal{I}_0)}_{b_{\text{curG}}A^0}, \quad (2.19)$$

where the above mentioned correspondence relations are marked explicitly, and where

$$\mathcal{I}_0 = \int_0^\infty (\eta - b_{\text{vol}}\rho) dr, \quad (2.20a)$$

$$\mathcal{I}_1 = \int_0^\infty (\eta - b_{\text{vol}}\rho) r dr, \quad (2.20b)$$

$$\mathcal{I}_2 = \int_0^\infty (\eta - b_{\text{vol}}\rho) r^2 dr, \quad (2.20c)$$

are radial moments associated with the nuclear surface layer. Relation (2.19) allows to find, among others, a dependence between the curvature, surface and Gauss-curvature terms that follow from the ETF method. To start,  $\eta$  and  $\rho$  are calculated from (2.1)-(2.2) using ETF method with Skyrme (SkM\*) forces of [32] wherefrom the integrals  $\mathcal{I}_0$ ,  $\mathcal{I}_1$  and  $\mathcal{I}_2$  are obtained. Next we proceed as follows: from Eq. (2.19), for each predefined value of  $b_{\text{cur}}$  we write down equality  $b_{\text{cur}}A^{2/3} = 8\pi R \cdot (\mathcal{I}_1 - \mathcal{I}_0 R)$  and, given  $\mathcal{I}_1$  and  $\mathcal{I}_0$ , we deduce the implied  $R$ -value. The latter quantity known, we insert it into  $b_{\text{surf}}A^{2/3} = 4\pi R^2 \cdot \mathcal{I}_0$  and  $b_{\text{curG}}A^0 = 4\pi \cdot (\mathcal{I}_2 - 2R\mathcal{I}_1 + R^2\mathcal{I}_0)$  and deduce  $b_{\text{surf}}$  and  $b_{\text{curG}}$ . Results of these operations are presented in Fig. 2 for  $^{100}\text{Sn}$  (top) and  $^{132}\text{Sn}$  (bottom) tin isotopes. It is seen from the figure that the surface energy becomes smaller when the curvature constant is growing. The radius constant corresponding to the leptodermous expansion and evaluated via relation  $R = r_0 A^{1/3}$  is marked on the right-hand side y-axis.

Finally let us observe the following interesting property. If we choose radius parameter  $R$  in such a way that the Gauss curvature term [cf. the last term in Eq. (2.19)] is minimal i.e.:

$$R = \frac{\mathcal{I}_1}{\mathcal{I}_0}, \quad (2.21)$$

then the first order curvature term [the second one in Eq. (2.19)] is equal to zero. Even though we are not going to impose this condition in what follows, it is instructive and helpful in analyzing the related description of the nuclear masses to know about the existence of the above correlation, especially when examining the role of the second-order (Gauss) curvature term.

The above observations confirm and illustrate the fact that the curvature terms in the nuclear energy are strictly related to the surface term as suggested in Sect. II A within a general introduction and that one can not discuss them separately. An increase of the first order curvature energy causes a decrease of the surface tension and *vice versa*. These observations will have consequences for the fitting procedures applied below.

### III. FITTING THE LIQUID DROP MODEL PARAMETERS

Our aim is to find the parameters of the liquid drop model which correspond to the leptodermous expansion of the nuclear energy [see Eq. (2.15)] and the Coulomb energy of a charged nuclear drop with a diffused surface. We are going to consider separately four variants of the liquid drop model: a. The one of Myers and Świątecki, Ref. [26], with its original fit of parameters, referred to as MS-LD; b. Similar to the above but with the newly fitted constants, the fit using the contemporary experimental data set and the microscopic energy corrections<sup>3</sup> - this variant is referred to as LDM; c. The modernized version of the liquid drop model that contains the Gauss-curvature term, is in the following referred to as 'new', NLD, and d. Similar to the above but containing the deformation-dependent first-order curvature term - this variant referred to as *Lublin-Strasbourg* version of the nuclear *Drop* energy formula, abbreviated to LSD.

We begin by presenting the main features of the liquid drop energy dependence on the surface-curvature terms.

#### A. Liquid Drop Masses with Curvature Terms: Characteristic Features

We assume, in accordance with the usual rules of the liquid drop model approaches, that the mass of an atom with  $Z$  protons,  $Z$  electrons and  $N$  neutrons is described by the following relation (cf. Refs. [26,18]):

$$\begin{aligned}
 M(Z, N; \text{def}) = & ZM_{\text{H}} + NM_{\text{n}} - 0.00001433 Z^{2.39} \\
 & + b_{\text{vol}} (1 - \kappa_{\text{vol}} I^2) A \\
 & + b_{\text{surf}} (1 - \kappa_{\text{surf}} I^2) A^{2/3} B_{\text{surf}}(\text{def}) \\
 & + b_{\text{cur}} (1 - \kappa_{\text{cur}} I^2) A^{1/3} B_{\text{cur}}(\text{def}) \\
 & + b_{\text{curG}} (1 - \kappa_{\text{curG}} I^2) A^0 \\
 & + \frac{3}{5} e^2 \frac{Z^2}{r_0^{\text{ch}} A^{1/3}} B_{\text{Coul}}(\text{def}) - C_4 \frac{Z^2}{A} \\
 & + E_{\text{micr}}(Z, N; \text{def}) + E_{\text{cong}}(Z, N),
 \end{aligned} \tag{3.1}$$

where

$$E_{\text{micr}} = E_{\text{pair}} + E_{\text{shell}} \tag{3.2}$$

is the microscopic energy containing the contributions from pairing and shell effects coming from the protons and from the neutrons. The congruence energy according to Ref. [18] is equal to:

---

<sup>3</sup>To be able to compare our results with those of the quoted authors, the microscopic energy corrections for the lightest nuclei, more precisely, those with  $Z < 29$  and  $N < 29$ , were taken from [18]; those for all heavier nuclei from [21].

$$E_{\text{cong}} = -10 \text{ MeV} \cdot \exp(-42 |I|/10) . \quad (3.3)$$

The term proportional to  $Z^{2.39}$  describes the binding energy of electrons. The surface diffuseness of the charge distribution reduces the Coulomb energy proportionally to  $Z^2/A$ .

In order to investigate the interplay between the Coulomb and nuclear energies when trying to reproduce the nuclear binding energies we have performed a test fit to the experimental data from Ref. [20] for various choices of the charge radius constant  $r_0^{ch}$ . The results are presented in Fig. 3, where several terms of the liquid drop model are plotted as functions of  $r_0^{ch}$ . The root-mean-square deviation of the binding energies,  $\langle \delta B \rangle$ , is shown referring to the right-hand side vertical axis. Surprisingly, the quality of the fit depends only slightly on the choice of  $r_0^{ch}$  but the magnitudes of the first and of the second order curvature terms change dramatically with  $r_0^{ch}$ . It is seen that for  $r_0^{ch} \approx 1.2$  fm both curvature terms are small since they both change sign near the above  $r_0^{ch}$ -value. (This Figure is similar to the previous one (Fig. 2) where the dependence of the surface and curvature terms on the radius of the leptodermous expansion was studied.)

The results in Fig. 3 show that it is rather difficult to fix the Coulomb radius parameter from the binding energies since the corresponding dependence is a flat function. Trying to deduce the related curvature contributions when varying both curvature terms is not very easy either, since the empirical  $r_0^{ch}$  value is expected not to differ very much from the mentioned special value of about 1.2 fm for which  $a_{\text{cur}}$  and  $a_{\text{curG}}$  are small (pass both through zero). This is precisely the type of parametric peculiarity of the macroscopic energy formula that has been mentioned in Sec. I. Under these conditions the fit to the fission barrier heights could give a valuable additional criterion. In the next Sections we are going to present the results of the fit of the parameters of the traditional (i.e without the curvature terms) liquid drop model energy expression to the experimental masses and the liquid drop model with the curvature terms where the parameters are adjusted either to both the measured ground state masses and fission barrier heights, or to the measured ground state masses only.

## B. New Parameters of the Traditional Myers-Świątecki Liquid-Drop Energy-Expression

Exactly the same mass expression as the one of Myers-Świątecki liquid drop (MS-LD) of Ref. [26]:

$$\begin{aligned} M(Z, N; \text{def}) = & ZM_{\text{H}} + NM_{\text{n}} - 0.00001433 Z^{2.39} \\ & + b_{\text{vol}} (1 - \kappa_{\text{vol}} I^2) A \\ & + b_{\text{surf}} (1 - \kappa_{\text{surf}} I^2) A^{2/3} \\ & + \frac{3}{5} \frac{e^2 Z^2}{r_0^{ch} A^{1/3}} - C_4 \frac{Z^2}{A} \\ & + E_{\text{def}}(Z, N) + E_{\text{pair}}(Z, N) + E_{\text{shell}}(Z, N) + E_{\text{cong}}(Z, N) , \end{aligned} \quad (3.4)$$

but with the microscopic corrections for deformation, pairing and shell effects treated as in Ref. [21] and the new estimate of the congruence energy ( $E_{\text{cong}}$ , Ref. [18]) was used to obtain the best fit to the 2766 empirical binding energies from Ref. [20] of the isotopes with

the proton and neutrons numbers larger or equal to 8. Following a practical recipe used in Ref. [18], when adjusting the parameters of the macroscopic model we take into account the nuclear deformations. In particular, the *macroscopic part* of the total energy,  $E_{\text{def}}$ , is taken from Tables of Ref. [21] ( $E_{\text{def}}$  is defined as the difference between the macroscopic energy of a nucleus at the equilibrium deformation and the energy of the same but spherical nucleus, plus the sum of the shell and pairing energies taken at the actual equilibrium deformation). The same approximation is used when fitting the parameter sets of other variants of the model presented in this paper.

The new set of parameters obtained by fitting the nuclear masses (but not using any information about the fission barriers, similarly as in Ref. [26]), is given below. For comparison the old values of the parameters taken from the above reference are given in parentheses:

$$b_{\text{vol}} = -15.8484 \quad (-15.667) \text{ MeV}, \quad (3.5a)$$

$$b_{\text{surf}} = 19.3859 \quad (18.56) \text{ MeV}, \quad (3.5b)$$

$$\kappa_{\text{vol}} = 1.8475 \quad (1.79), \quad (3.5c)$$

$$\kappa_{\text{surf}} = 1.9830 \quad (1.79), \quad (3.5d)$$

$$r_0^{ch} = 1.18995 \quad (1.2049) \text{ fm}, \quad (3.5e)$$

$$C_4 = 1.19949 \quad (1.21129) \text{ MeV}. \quad (3.5f)$$

The r.m.s. mass deviation corresponding to the new set of parameters and the microscopic corrections from Ref. [21] is  $< \delta M > = 0.732 \text{ MeV}$ ; an analogous quantity for the old set of the liquid drop parameters and the same microscopic corrections is  $< \delta M > = 4.477 \text{ MeV}$ . The r.m.s. mass deviation obtained with the new parameter set is comparable with the one of the Thomas-Fermi model ( $< \delta M > = 0.757 \text{ MeV}$ ) and proves that the liquid drop approximation can reproduce the nuclear masses with a comparably high accuracy.

Let us observe that *neither* the old set of the liquid drop parameters (MS-LD) *nor* the new one (LDM) is able to reproduce correctly the magnitudes of the experimental fission barriers. The discrepancies between theoretical and experimental fission barrier heights of 40 nuclei that can be found in the published literature<sup>4</sup> are presented in Fig. 4 (for the sources cf. Refs. [18,22,33] and references quoted there). To extract the barrier heights from the experimental data we have used a similar prescription as the one in Ref. [22], namely we define the barrier height as a difference between the liquid drop saddle-point energy and the ground state energy deduced from the ground-state masses. It is seen in Fig. 4 (top) that the traditional Myers-Świątecki liquid drop (MS-LD) model *overestimates* the barrier heights of the lighter nuclei by about 10 MeV and by about 3-4 MeV those of the heavier

---

<sup>4</sup>In this paper we use only those experimental barrier heights that can be found in the published sources; they correspond to 40 nuclei with  $75 \leq A \leq 252$ . This information concerns four relatively light nuclei *viz.*  ${}^{75}_{35}\text{Br}$  and  ${}^{90,94,98}_{40}\text{Mo}$  and the whole rest of nuclei clearly separated in terms of  $Z$  ( $Z > 70$ ). The barriers of these four lightest nuclei present the same type of difficulties for all the variants of the model, including the one introduced in this paper (LSD). As far as the barriers of  $Z > 70$  nuclei are concerned, some variants of the model describe them very well, some variants are clearly less satisfactory (for details see below).

ones. Our new fit of parameters of this traditional liquid drop model (LDM) overestimates the barrier heights even more significantly (Fig. 4, bottom). Does it mean that the liquid drop model is unable to reproduce with a more respectable accuracy the positions of the fission saddle-point energies? In order to answer this question we have performed additional tests in which we have made either a simultaneous fit of the liquid drop model parameters to the experimental masses and fission barrier heights, or the fits limited to the nuclear masses. The results are presented in the next Sections.

### C. Liquid Drop Model with Curvature Terms

The purpose of the following discussion is to examine the influence of the two curvature terms introduced earlier through relations (2.14) and (3.1). We would like to adjust the parameters of the curvature-extended liquid drop model both to the huge body of the experimental nuclear binding energies *known today* and, if necessary, to the experimental fission barrier heights - in this context we are going to profit from the observations presented in Sect. III A. The nuclear mass expression of Eq. (3.1), compared to the one by Myers and Świątecki in Eq. (3.4), contains the curvature terms of the first and of the second orders. The fit to the experimental masses and fission-barrier heights will be performed in three different ways: the one where only the second order curvature term was included, another one with the first and the second order curvature terms, and finally the one with the first order curvature term only. In particular it will be shown that taking into account the Gauss-curvature (second-order) term which is  $A$  and deformation independent but may possibly introduce a strong dependence on the isospin factor  $I = (N - Z)/(N + Z)$ , improves the quality of the mass fit provided the surface tension and related coefficients were fitted to the fission barriers. It influences indirectly the fission barrier heights through an extra  $(Z, N)$ -dependence in all other simultaneously fitted parameters.

We proceed to discuss the results of the three variants of the fitting procedure separately.

#### 1. Gauss-Curvature Term

In order to study the effect of the Gauss-curvature term alone on the liquid drop energy expression we set the first order curvature term to zero,  $b_{\text{cur}} = 0$ , thus assuming for the moment that the barrier heights can be described by the competition between the surface and Coulomb contributions only, very much like in the traditional liquid drop model approaches. When discussing the particular case of spherical nuclei (but the conclusions drawn apply to some extent to the moderately deformed nuclei as well) it was shown, cf. Eqs. (2.18 - 2.20), that if one sets  $b_{\text{cur}} = 0$  then necessarily  $b_{\text{curG}} \neq 0$ .

To fit the parameters of the model in this case, we use the fact that only some of them influence the fission barriers and we proceed as follows. First, for each value of the charge radius ( $r_0^{ch}$ ), we fix the surface coefficients  $b_{\text{surf}}$  and  $\kappa_{\text{surf}}$ , by making the least square fit to all *experimental fission barrier heights* listed in Ref. [18]. Then the charge radius and all other than the surface-tension LDM parameters in Eq. (3.1), including the Gauss-curvature term, are adjusted by the least square fit to the *experimental binding energies* of 2766 isotopes with  $Z, N \geq 8$  taken from Ref. [20].

The parameters of such a '*new*' *liquid drop* (NLD) formula are listed in Table I. The mean square deviation of the theoretical and experimental binding energies,  $\langle \delta B \rangle = 0.814$  MeV, is only slightly larger than that of  $\langle \delta B \rangle = 0.732$  MeV, obtained with the re-fitted parameters of the traditional Myers-Świątecki liquid drop model (LDM) as described in Sect. III B. However, the fission barrier heights are now much better reproduced. The r.m.s. deviation of the barrier heights for all treated nuclei is  $\langle \delta V_B \rangle = 1.90$  MeV while for the LDM we found  $\langle \delta V_B \rangle = 7.08$  MeV (see in Fig. 4). Including the isospin-dependent Gauss-curvature term improves the agreement with the experimental barrier heights, nevertheless the corresponding new set of parameters does not reproduce perfectly the barriers: it is seen in Fig. 5, top, that the barriers of the light isotopes ( $A < 100$ ) are *overestimated* by about 4 MeV and the barriers of nuclei with  $A \sim 180$  are *underestimated* by about 3 MeV while the barrier heights of the heaviest nuclei are *overestimated* by 1.5 MeV. Thus our procedure provides, on the average, an improved fit to the experimental fission barrier heights but it does not reproduce very well neither  $Z^2/A$  nor  $A$  dependence of them.

Below we show that a possible remedy is to include the first order curvature term.

## 2. Both Curvature Terms

It is known that the light nuclei have saddle points at very elongated shapes whereas the saddle points in the actinide and trans-actinide nuclei correspond to rather compact shapes. The surface and curvature terms depend on deformation in a very similar way for small and even moderate deformations [38], while at large deformations the differences become pronounced. This feature will be used to improve the description.

Performing the least square fit to the experimental fission barrier heights for a fixed charge radius ( $r_0^{ch}$ ) we have obtained the surface,  $b_{\text{surf}}$  and  $\kappa_{\text{surf}}$ , and the curvature,  $b_{\text{cur}}$  and  $\kappa_{\text{cur}}$  coefficients, all other parameters being insensitive to the barriers. The charge radius constant as well as the rest of the parameters of the deformation independent terms in Eq. (3.1) were obtained as before by the least square fit to the known experimental masses of Ref. [20]. The r.m.s. deviation from the experimental data obtained with such a procedure is 0.844 MeV for 2766 masses and only 1.06 MeV for the fission barriers. The parameters obtained through this procedure give a very strong dependence of both curvature terms on the reduced isospin, i.e. the corresponding  $\kappa$ -coefficients are large. We find:  $b_{\text{cur}} = -8.219$  MeV,  $\kappa_{\text{cur}} = 38.92$  and  $b_{\text{curG}} = 21.82$  MeV,  $\kappa_{\text{curG}} = 25.0$ . This dependence leads to the negative first order curvature contribution for the light nuclei ( $A < 130$ ) (recall that the corresponding contribution is  $b_{\text{cur}}(1 - \kappa_{\text{cur}}I^2)$ , and thus for  $I^2$  small, the total contribution of this term is negative).

The next attempt, while using the fitting procedure that employs both curvature terms was to fit all 10 parameters of the model, Eq. (3.1), to the experimental binding energies *only*. This lead to the r.m.s. deviation from the experimental masses equal to 0.693 MeV, but the fission barriers obtained in this way were up to 20 MeV too high for the light nuclei with  $A < 100$  while for the heaviest nuclei they were by about 2 MeV too small. These unsatisfactory results lead us to examine more thoroughly the use of the first order curvature term only i.e. by setting by definition the Gauss curvature term to zero, as discussed in the following section.



### 3. First Order Curvature Term and the LSD Parameter Set

It turns out that the liquid drop model which in addition to the volume, surface and Coulomb terms contains only the first order curvature term gives the most satisfactory results, as presented below. The parameters of this *Lublin-Strasbourg Drop* (LSD) variant of the macroscopic model are fitted solely to the nuclear masses and not to the fission barriers. The LSD parameters obtained by fitting to the 2766 experimental masses of Ref. [20] are listed in Table I. The differences between the theoretical and experimental barrier heights are presented in Fig. 5, bottom. Now the mean square deviation of the binding energies amounts to  $\langle \delta B \rangle = 0.698$  MeV, while the mean square deviation of the barrier heights  $\langle \delta V_B \rangle = 3.56$  MeV, but it decreases to only 0.88 MeV when the four lightest nuclei are disregarded i.e. when only the nuclei with  $Z > 70$  are considered.

As it is seen the parameterization of the barrier heights for heavier nuclei with  $Z > 70$  is improved considerably. The fission barriers obtained with the LSD model are closer to the experimental ones as compared to analogous results obtained in Ref. [18] with the Thomas-Fermi model (MS-TF); this is illustrated in Fig. 6, top. The difference between the MS-TF and the measured barriers are plotted in the bottom part of Fig. 6. It is seen that for heavier nuclei the agreement between the experimental data and the LSD fission barriers (Fig. 5, bottom) is even better than that for the MS-TF model while for the light isotopes ( $A < 100$ ) both models give comparable fission barriers, approximately 10 MeV too high. This large discrepancy between the theoretically predicted fission barrier heights and the measured values for light nuclei could originate from the fact that these fission barriers are very broad and the saddle points are very close to the scission points. At such configurations it could happen that the negative congruence energy (nearly) doubles, as suggested in Ref. [18], and as a consequence the fission barrier heights calculated within such an approach could get much closer the experimental ones; here we do not examine this type of effects since the microscopic origin of the congruence effects exceeds the framework of the classical model.

The role of the curvature term together with its dependence on isospin needs to be still analyzed in more detail. We shall examine the above questions in the next Section.

The calculated LSD masses of 2766 nuclei are compared with the measured ones in Fig. 7. The lines join the points corresponding to the common-isotope chains. A part of the observed local discrepancies may originate from the microscopic corrections to the macroscopic energies that were evaluated in Ref. [21] assuming the same deformations for the proton and neutron distributions. The self-consistent calculations made in Ref. [36,37] show that in the ground state the proton and the neutron distributions are not equally deformed. A rough estimate made in Ref. [39] within the Hartree-Fock-Bogolubov approximation with the Gogny force shows that this effect can change the ground state energy by approximately  $\pm 0.5$  MeV. The effect of deformations that are different for the proton and neutron distributions can be incorporated to the macroscopic-microscopic models by introducing an additional term; this aspect is not going to be developed in the present paper. The form and magnitude of the term responsible for the change of the macroscopic energy due to the deformation difference of both kinds particles was estimated in Ref. [40] within the extended Thomas-Fermi model with the Skyrme forces.

To estimate the 'performance stability' of a given parameter-fit it is instructive to ex-

amine, among others, how a given mass formula fitted to a certain 'narrow' mass range performs in an extended mass range and *vice versa*. For instance, with the LSD parameter set fitted to 1654 isotopes from the Audi-Wapstra tables we may predict the 2776 masses corresponding to the compilation of Anthony and by taking the corresponding differences we may calculate the implied r.m.s. deviations that illustrates the 'predictive power' of the model and its parametrisation. Such a comparison is presented in Table II for the LSD parameter set as well as for two other models indicated. For comparison also an inverse test has been examined i.e. estimating the performance quality when going from a broader mass range to a narrower one. Results in Table II indicate among others a remarkable stability or 'predictive power' of the LSD approach: by fitting the parameters to the 1654 masses and predicting the result for the 2776 masses, we obtain the r.m.s. deviation of 0.711 MeV, i.e. only 13 keV worse than the direct fit to the 2776 masses, the latter giving the r.m.s. of 0.698 MeV.

#### IV. FISSION BARRIERS AND PROPERTIES OF THE POTENTIAL ENERGY SURFACES AROUND THE SADDLE POINTS

Fission barrier heights obtained with the help of the curvature-dependent liquid drop (LSD) model have been compared with the experimental data and with the estimates of the Myers-Świątecki liquid drop (MS-LD) formula [26], in Figs. 4 and 5. In both models the fission barrier heights were defined as differences between the LD masses at the saddle point deformations and the ground state masses. Such a prescription for the barrier heights was used also in Refs. [18,22], where the authors argued (the so called 'topological property') that the shell corrections at the saddle points should be small. From Fig. 5 it is seen that the fission barriers obtained with the LSD parameter set are very close to the measured values taken from Refs. [18,33,22] and references cited there, but also that they are systematically overestimated for nuclei with  $Z > 70$  as it was the case of the traditional MS-LD, Ref. [26], model. The LSD barrier heights are also close to those obtained within the Thomas-Fermi model of Myers and Świątecki what is seen in Fig. 6, top.

Such an agreement was possible only due to the presence of the first order curvature term in the LSD formula. As it can be seen from Table I, the LSD curvature energy grows with reduced isospin  $I = (N - Z)/A$  while the magnitude of the volume and surface terms decreases with  $I$ . Without such an  $I$ -dependence of the surface and curvature terms it would have not been possible to reproduce the whole systematics of the barrier heights (it will shown below, Fig. 11, that such a strong dependence is very similar in the ETFSI approach indicating that this particular result of the fit should not be taken as surprise but rather as an argument of the physical correctness of the LSD approach).

One extra remark will be in place here corresponding to the magnitude of the curvature coefficient (see also comments related to Eq. (2.9b)). Our parameterization in terms of  $b_{\text{cur}}$  corresponds more to the discussions usually associated with the LD energy expression rather than the one used in the microscopic-type approaches. The correspondence between the two type of parameterizations has the form

$$\begin{aligned} b_{\text{surf}} [1 - \kappa_{\text{surf}} I^2] A^{2/3} + b_{\text{cur}} [1 - \kappa_{\text{cur}} I^2] A^{1/3} \\ \rightarrow a_{\text{surf}} A^{2/3} + [a_{\text{cur}} - 2a_{\text{surf}}^2/K] A^{1/3}, \end{aligned} \quad (4.1)$$

where  $K$  denotes the nuclear matter incompressibility coefficient and the corresponding term represents the semi-infinite nuclear matter contribution. Even if the isospin dependence in the second line in the above relation would have been taken into account the above expression makes it clear that the direct comparison between the curvature coefficients when using these two parameterizations cannot be made. However, the factor proportional to  $a_{\text{surf}}^2$  is of the order of 3 MeV and for  $a_{\text{cur}} \approx 7$  MeV the corresponding expression will correspond to the fitted  $b_{\text{cur}}$  values. This estimate can be further detailed by using some literature results: Ref. [31] quotes the estimate  $a_{\text{cur}} \approx 11$  MeV, while Ref. [12]  $a_{\text{cur}}$  ranging from 9.52 to about 13 MeV as obtained with the six representative Skyrme interactions; one may conclude that our fit result and the quoted microscopic model results have comparable orders magnitude, our numbers being slightly smaller.

It is interesting to compare the fission barrier profiles obtained with different parameter sets of the liquid drop model. In Fig. 8 the fission barriers obtained with the traditional Myers-Świątecki (MS-LD), with the new Gauss-curvature dependent (NLD), and that with the first-order curvature term (LSD) liquid drop models are plotted for  $^{232}\text{Th}$  (top) and  $^{240}\text{Pu}$  (bottom). It is seen that in spite of the differences in the barrier heights the slopes from the saddle to scission points are similar in all three approaches. The barriers are plotted as functions of distance  $R_{12}$  (in  $R_0$  units) between the fission fragments. Each barrier point was minimized with respect to all even  $\beta_\lambda$  deformations with  $\lambda \leq 14$ .

The neutron number dependence of the fission barriers of Yb isotopes evaluated with the MS-LD and LSD parameter sets are presented in Fig. 9. This nuclear range is of particular interest for the hyperdeformation studies and several, so far unsuccessful experimental tests have been already attempted. Each curve is drawn up to the deformation point close to the scission point. It is seen that the LSD barrier heights are a few MeV smaller than those of MS-LD model and that they grow less significantly with neutron number. Also the MS-LD barriers are shorter than the LSD ones. The fission barrier profiles and their correct description together with the saddle-to-scission path-length are important when studying the properties of e.g. super- or hyper-deformed nuclei. In this paper we are not going to go into more details leaving the corresponding discussion to a forthcoming paper. Instead we would like to examine and illustrate on some examples the stiffness of the potential energy surface with respect to higher multipolarity deformations for the elongations which are close to the saddle and/or scission configurations. This aspect is very important in the studies of e.g. multi-path fission mechanisms where the shell energies corresponding to the relatively exotic (e.g. high-multipolarity) deformations may provide competitive fission mechanisms. Such a problem arises also at high spins and therefore will also become important for the new generation of the calculations aiming at the hyper-deformation effect. In Fig. 10 the cross sections of the potential energy surfaces obtained with the MS-LD and LSD approaches on the one hand, and with the Yukawa-Folded energy expression with parameters from [25] on the other hand, are plotted for  $^{172}\text{Yb}$  at  $\beta = 2$  as functions of  $\beta_4$  (top),  $\beta_6$  (middle) and  $\beta_8$  (bottom). It is seen that the stiffness properties with respect to these deformations are almost the same in the case of the first two compared models. The YF approach cannot distinguish in any significant manner between, say,  $\beta_4 = 0.5$  and  $\beta_4 = 1.0$  (the corresponding energy difference is smaller than 1 MeV compared to about 5 MeV in the case of the other two approaches) and varies only weakly in terms of the higher order multipoles. This very strong indifference of the YF approach with respect to significant variations of the nuclear

surface at strong elongations was considered for some time already as a weakness of the latter approach, cf. Ref. [24].

In Fig. 11 the fission barrier heights of several Fm isotopes calculated with the LSD and NLD sets of parameters are compared with the fission barrier heights obtained in Ref. [23] within the extended Thomas-Fermi model with the Skyrme interaction (ETFSI). It is seen that the barrier heights obtained with the NLD and LSD parameters are close to each other for the light Fm isotopes while for the heaviest ones one may notice a significant (3 MeV) difference between the two families of the barrier heights. This decrease of the barrier heights with increasing neutron number  $N$  obtained in the LSD model for heavy Fm isotopes is confirmed by the ETFSI results [23].

The logarithms of the experimental life-times,  $T_{sf}$ , are plotted for comparison, in Fig. 12. It is known from the macroscopic-microscopic type of calculations that it was almost impossible to reproduce the spontaneous fission life time ( $T_{sf}$ ) systematics for the chain of Fm isotopes. For the majority of the theoretical calculations, the spontaneous fission life times of heavier Fm isotopes are too long while for the light and medium-heavy isotopes they are relatively well reproduced. An attempt in Ref. [41], within the macroscopic model that contained no curvature terms confirmed the existence of the same deficiency. Such a discrepancy in the systematics originates probably from too strong  $N$ -dependence of the macroscopic fission barrier heights; a new parametrisation can be seen as a step into a right direction.

## V. SUMMARY

We have shown that it is possible to reproduce simultaneously and with a reasonable precision the ground-state binding-energies and fission barrier heights of nuclei within the liquid drop model containing the first and/or the second order curvature terms. Out of three variants of the model discussed in detail in this paper the one abbreviated LSD (Lublin-Strasbourg Drop) offers the highest precision in the description of masses and fission barriers; it also has a remarkable stability property with respect to extrapolation from narrower to the broader range of nuclei.

The traditional (i.e. without the curvature terms) liquid drop model energy expression, abbreviated LDM, with the parameters adjusted to the experimental masses only, reproduces remarkably well the experimental masses but gives the barrier heights about (3 to 15) MeV bigger than their measured values.

The liquid drop model with parameters fitted simultaneously to the experimental binding energies and barrier heights can reproduce rather well both types of data when it contains the  $A$ -independent (but isospin-dependent) second order curvature (Gauss) term. This almost traditional expression, i.e. without the first order curvature terms, but with the surface tension adjusted to the experimental barrier heights, abbreviated NLD, reproduces *on the average* the right positions of the saddle points but gives a rather poor *systematic dependence* of the barrier heights on  $Z^2/A$ .

The LSD variant of the liquid drop model contains the term proportional to  $A^{1/3}$  (first-order curvature-term) and no Gauss-curvature term. It can reproduce the experimental binding energies and the fission barrier heights with an accuracy comparable to- or better

than the Thomas-Fermi model of Ref. [18], or the HF+BCS model with Skyrme forces of Ref. [23]. Perhaps surprisingly, its parameters are adjusted to the experimental binding energies only - no information about the fission barriers has been used to fit the LSD variant parameters. Yet, it gives a correct description of the masses and the fission barriers, with the performance comparable to or better than that of other models. It gives simultaneously the right *systematic* of the barrier heights for the isotopes with  $Z > 70$ . The most important information about these results is contained in Tables I and II of the paper.

Similarly as in the Thomas-Fermi model of Ref. [18] the LSD fission barriers of the lighter nuclei ( $A < 100$ ) are overestimated by about 10 MeV. Here our conclusions coincide with those of [22] where the concept of the congruence mechanism has been discussed to remedy this problem. The isospin dependence of the surface and curvature terms in the LSD energy expression is qualitatively confirmed by the systematic of the spontaneous fission life times of Fermium isotopes and quantitatively by the results of the ETFSI model.

In parallel with completing this study, an extension of the present considerations to the case of the nuclear rotation has been examined and a number of independent tests of performance of the LSD variant of the model through comparison to the measured barrier heights at high angular momenta has been advanced. An agreement with the results on fission barriers for a few rotating nuclei has been found comparable to the one discussed in this paper for the static case [42].

## ACKNOWLEDGMENTS

One of the authors (K. P.) wishes to express his thanks for the warm hospitality extended to him by the Institute for Subatomic Research (IReS) and the Louis Pasteur University of Strasbourg; he is particularly indebted to the French Ministry of National Education for the invitation as *P.A.S.T.* guest professor that enabled the present collaboration.

## APPENDIX A: A SHORT SUMMARY OF THE THOMAS-FERMI MODEL OF MYERS AND ŚWIĄTECKI

In Ref. [18] the Thomas-Fermi model was applied to a nucleus in which the nucleons interact via modified Seyler-Blanchard [34] forces:

$$v_{12} = \frac{2T_0}{\rho_0} \cdot Y(r_{12}) \cdot \left[ -\alpha + \beta \left( \frac{p_{12}}{P_0} \right)^2 - \gamma \frac{P_0}{p_{12}} + \sigma \left( \frac{2\bar{\rho}}{\rho_0} \right) \right]. \quad (\text{A1})$$

Here  $T_0$ ,  $P_0$  and  $\rho_0$  are the Fermi energy, the Fermi momentum and the nuclear matter density, respectively. The function  $Y(r_{12})$  describes the Yukawa and Coulomb interactions:

$$Y(r_{12}) = \frac{1}{4\pi a^3} \frac{e^{r_{12}/a}}{r_{12}/a} + V_{\text{Coul}}. \quad (\text{A2})$$

and  $\bar{\rho}$  is the average of the densities of particles "1" and "2":

$$\bar{\rho}^{2/3} = (\rho_1^{2/3} + \rho_2^{2/3})/2. \quad (\text{A3})$$

The mass defect is described by the following expression:

$$\Delta M(N, Z) = ZM_{\text{H}} + NM_{\text{n}} + E_{\text{TF}} - 0.00001433 Z^{2.39} + E_{\text{shell}} + E_{\text{pair}} + E_{\text{cong}} . \quad (\text{A4})$$

The corrections for the shell, pairing and deformation effects are taken from the tables of Moeller [21]. The congruence energy according to Ref. [18] is equal to:

$$E_{\text{cong}} = -10 \text{ MeV } \exp(-42|I|/10) . \quad (\text{A5})$$

The Thomas-Fermi mass expression depends finally on the range of Yukawa forces  $a$  and six adjustable parameters  $\xi, \zeta, \alpha, \beta, \gamma, \sigma$  *via*

$$\alpha_{\ell,u} = \frac{1}{2}(1 \mp \xi)\alpha , \quad (\text{A6a})$$

$$\beta_{\ell,u} = \frac{1}{2}(1 \mp \zeta)\beta , \quad (\text{A6b})$$

$$\gamma_{\ell,u} = \frac{1}{2}(1 \mp \zeta)\gamma , \quad (\text{A6c})$$

$$\sigma_{\ell,u} = \frac{1}{2}(1 \mp \zeta)\sigma , \quad (\text{A6d})$$

where  $\ell, u$  refer to 'like' and 'unlike', and are associated with the minus and plus signs, respectively.

The least square fit done for 1654 isotopes approximates the nuclear masses with the r.m.s. deviation  $< \delta M > = 0.655 \text{ MeV}$ .

## REFERENCES

- [1] C. F. von Weizsäcker, Z. Phys. **96**, 431 (1935).
- [2] H. A. Bethe, R. F. Bacher, Rev. Mod. Phys. **8** 82 (1936).
- [3] L. Meitner, O. R. Frisch, Nature **143**, 239 (1939).
- [4] N. Bohr, J. A. Wheeler, Phys. Rev. **56**, 426 (1939).
- [5] D. L. Hill, J. A. Wheeler, Phys. Rev. **89**, 1102 (1953).
- [6] H. v. Groote, E. Hilf, Nucl. Phys. **A129**, 513 (1969).
- [7] K. A. Brueckner, J. R. Buchler, S. Jorna, R. J. Lombard, Phys. Rev. **171**, 1188 (1969).
- [8] W. D. Myers, W. J. Świątecki, Ann. Phys. **55**, 395 (1969).
- [9] W. Stocker, Nucl. Phys. **A215**, 591 (1973).
- [10] B. Grammaticos, Z. Phys. **A312**, 99 (1983).
- [11] W. Stocker, J. Bartel, J. R. Nix, A. J. Sierk, Nucl. Phys. **A489**, 252 (1988).
- [12] M. Brack, C. Guet, H.-B. Høkanesson, Phys. Rep. **123**, 276 (1984).
- [13] M. Durand, P. Schuck, X. Viñas, Z. Phys. **A346**, 87 (1993).
- [14] M. Centelles, X. Viñas, Nucl. Phys. **A536**, 173 (1993).
- [15] M. Centelles, X. Viñas, P. Schuck, Phys. Rev. **C53**, 1018 (1996).
- [16] D. von Eiff, W. Stocker, M. K. Weigel, Phys. Rev. **C50**, 1436 (1994).
- [17] F. Douchin, P. Haensel, J. Meyer, Nucl. Phys. **A665**, 419 (200).
- [18] W. D. Myers, W. J. Świątecki, Nucl. Phys. **A601**, 141 (1996).
- [19] G. Audi, A. H. Wapstra, Nucl. Phys. **A565**, 1 (1993).
- [20] M. S. Antony, Chart of Nuclides, Strasbourg 2002, in preparation.
- [21] P. Möller, J. R. Nix, W. D. Myers, W. J. Świątecki, At. Data Nucl. Data Tables **59**, 185 (1995).
- [22] W. D. Myers, W. J. Świątecki, Phys. Rev. **C60**, 014606 (1999).
- [23] F. Tondeur, S. Goriely, J. M. Pearson, M. Onsi, Phys. Rev. **C62** (2000) 024308; S. Goriely, J.M. Pearson, and F. Tondeur, At. Data and Nucl. Data Tables **77**, 311 (2001).
- [24] L.-O. Jönsson, Nucl. Phys. **A608**, 1 (1996).
- [25] P. Möller and J. R. Nix, . At. Data Nucl. Data Tables **26**, 165 (1981).
- [26] W. D. Myers, W. J. Świątecki, Ark. Phys. **36**, 343 (1967); W. D. Myers, W. J. Świątecki, Nucl. Phys. **81**, 1 (1966).
- [27] H. J. Krappe, J. R. Nix, A. J. Sierk, Phys. Rev. **C20**, 992 (1979).
- [28] A. J. Sierk, Phys. Rev. **C33**, 2039 (1986).
- [29] S. Trentalange, S. E. Koonin, A. J. Sierk, Phys. Rev. **C22**, 1159 (1980).
- [30] W. D. Myers, W. J. Świątecki, Ann. Phys. **84**, 186 (1974).
- [31] W. D. Myers, W. J. Świątecki, Ann. Phys. **2044**, 401 (1990).
- [32] J. Bartel, P. Quentin, M. Brack, C. Guet, H.-B. Høkanesson, Nucl. Phys. **A386**, 79 (1982).
- [33] K. X. Jing, L. G. Moretto, A. C. Veeck, N. Colonna, I. Lhenry, K. Tso, K. Hanold, W. Skulski, Q. Sui, G. J. Wozniak, Nucl. Phys. **A645**, 203 (1999).
- [34] R. G. Seyler, C. H. Blanchard, Phys. Rev. **124**, 227 (1961); **131**, 355 (1963).
- [35] A. Mamdouh, J. M. Pearson, M. Rayset, F. Tondeur, Nucl. Phys. **A679**, 337 (2001).
- [36] K. Pomorski, P. Ring, G. A. Lalazissis, A. Baran, Z. Łojewski, B. Nerlo-Pomorska, M. Warda, Nucl. Phys. **A624**, 349 (1997).
- [37] M. Warda, B. Nerlo-Pomorska, K. Pomorski, Nucl. Phys. **A635**, 484 (1998).

- [38] R. W. Hasse, W. D. Myers, Geometrical Relationships of Macroscopic Nuclear Physics, Springer Verlag, Berlin 1988.
- [39] J. F. Berger, K. Pomorski, Phys. Rev. Lett. **85**, 30 (2000).
- [40] A. Dobrowolski, K. Pomorski, J. Bartel, Phys. Rev. **65**, 041306(R) (2002).
- [41] Z. Łojewski, A. Staszczak, Nucl. Phys. **A657**, 134 (1999).
- [42] B. Herskind, private communication, 2002.



# TABLES

TABLE I. The parameters of the liquid drop model fitted to the measured atomic masses only (LDM and LSD) and to experimental barriers heights and masses (NLD).

Term	Units	LDM	NLD	LSD
$b_{\text{vol}}$	MeV	-15.8484	-15.4721	-15.4920
$\kappa_{\text{vol}}$	-	1.8475	1.6411	1.8601
$b_{\text{surf}}$	MeV	19.3859	17.0603	16.9707
$\kappa_{\text{surf}}$	-	1.9830	0.7546	2.2938
$b_{\text{cur}}$	MeV	-	-	3.8602
$\kappa_{\text{cur}}$	-	-	-	-2.3764
$b_{\text{curG}}$	MeV	-	10.3574	-
$\kappa_{\text{curG}}$	-	-	13.4235	-
$r_0$	fm	1.18995	1.21610	1.21725
$C_4$	MeV	1.1995	0.7952	0.9181
$\langle \delta B \rangle$	MeV	0.732	0.814	0.698
$\langle \delta V_B \rangle$	MeV	7.08	1.90	3.56
$\langle \delta V_B \rangle (Z > 70)$	MeV	5.58	1.56	0.88

TABLE II. Root means square deviations (in MeV) of the theoretical and the experimental binding energies of isotopes with  $Z, N \geq 8$ . The experimental masses are taken from the Audi-Wapstra tables (1654 isotopes) and from Anthony compilation (2766 isotopes). In the first column the numbers of experimental masses are indicated as used when fitting the parameters for the LSD variant of the present article as well as for the Thomas-Fermi and Hartree-Fock with Skyrme parameter set *MSk7*. The second and third columns contain the performance test and the 'extrapolation test' for the fits with the numbers of masses given in the head of those columns.

Model	r.m.s (2766)	r.m.s. (1654)
LSD(2766)	0.698	0.610
LSD(1654)	0.711	0.600
TF-MS(1654)	0.757	0.655
MSk7(1888)	0.828	0.738

# FIGURES

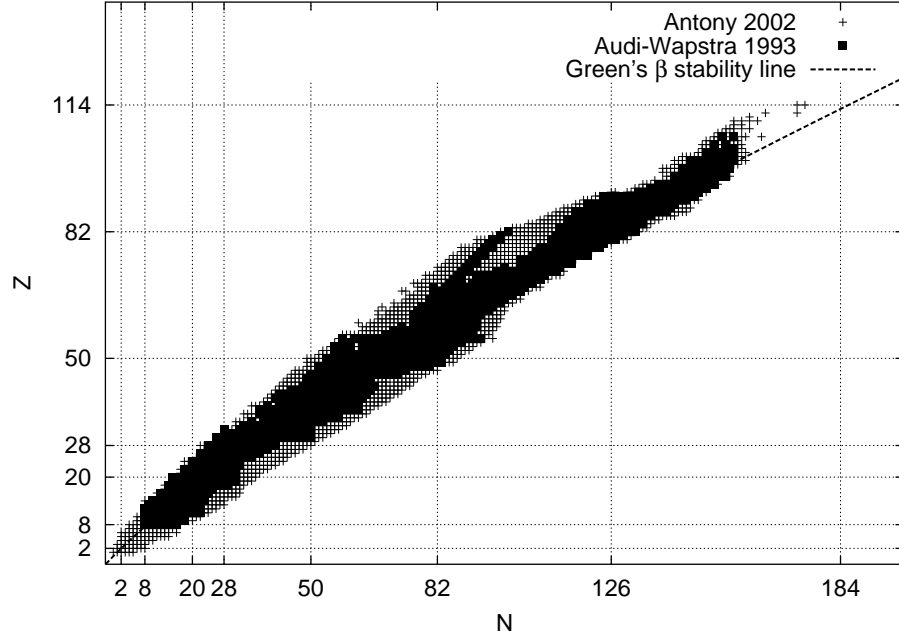


FIG. 1. The chart of isotopes for which the experimental binding energies are known. The crosses correspond to data from the compilation of Anthony [20] while black squares to the data from Ref. [19] on basis of which the analysis of Myers and Świątecki [18] was done.

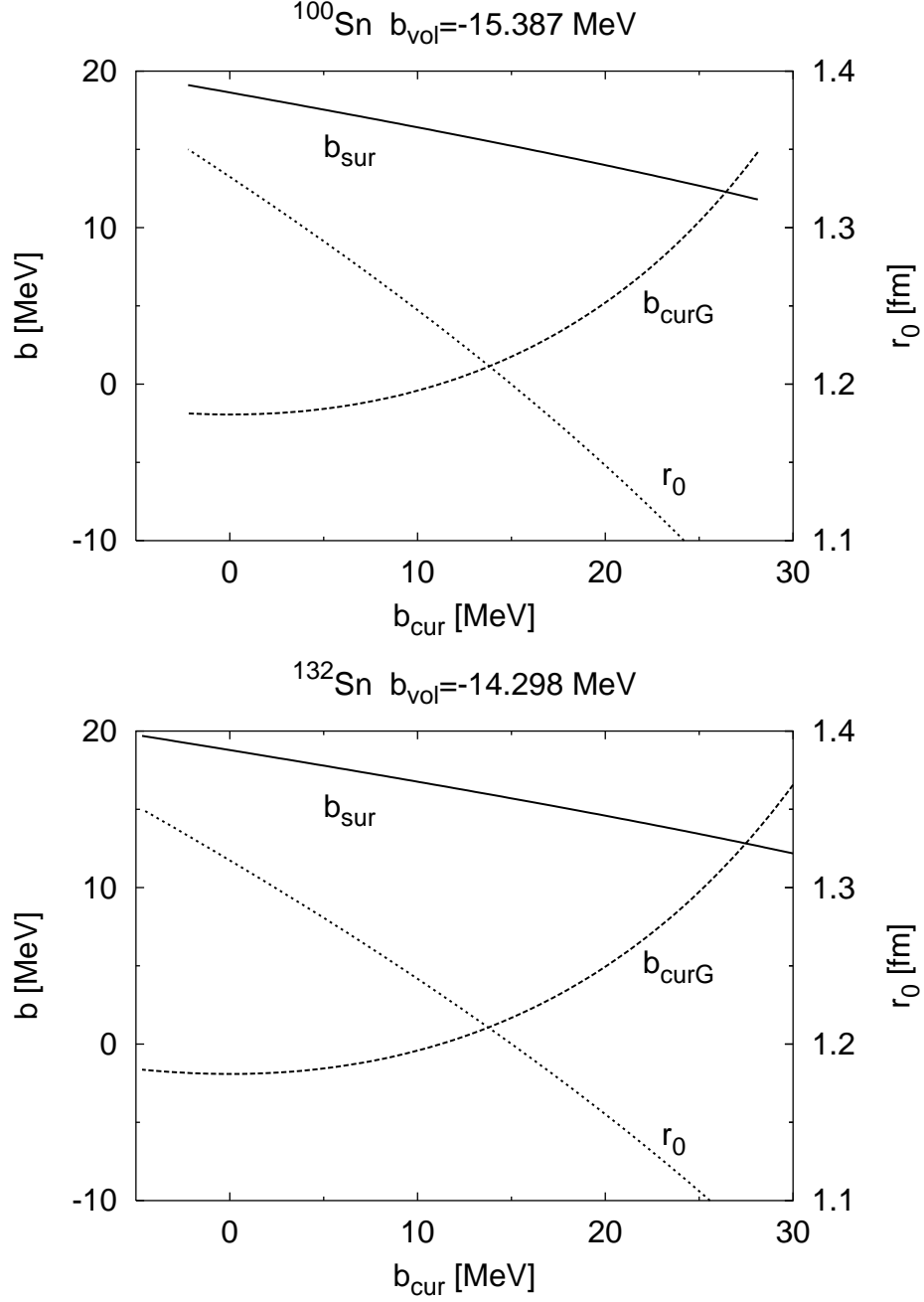


FIG. 2. Interplay between the total value of the first order curvature ( $b_{\text{cur}}$ ), the surface ( $b_{\text{surf}}$ ) and the second order (Gauss) curvature ( $b_{\text{curG}}$ ) terms evaluated in the leptodermous expansion around  $R = r_0 A^{1/3}$  of the ETF energy functional obtained with the Skyrme forces (SkM\*) for  $^{100}\text{Sn}$  (top) and  $^{132}\text{Sn}$  (bottom). The corresponding values of  $r_0$  refer to the right-hand side ordinate axis.

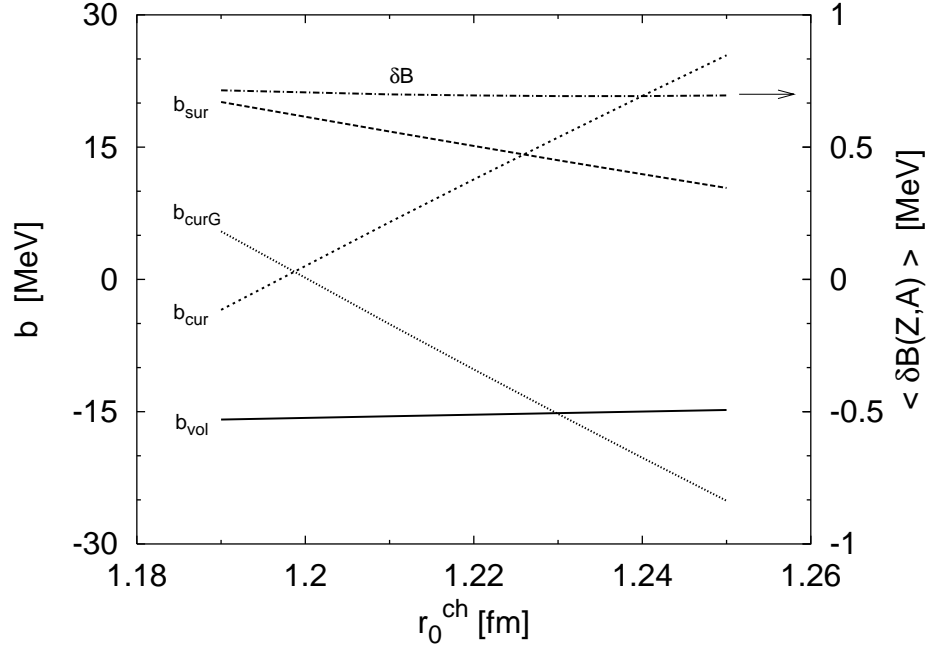


FIG. 3. Dependence of various liquid drop model terms obtained by the least square fits to the experimental masses as functions of the Coulomb radius constant  $r_0^{\text{ch}}$ . The corresponding r.m.s. deviation of the differences between the theoretical and experimental binding energies  $\langle \delta B \rangle$  refers to the right-hand side ordinate axis.

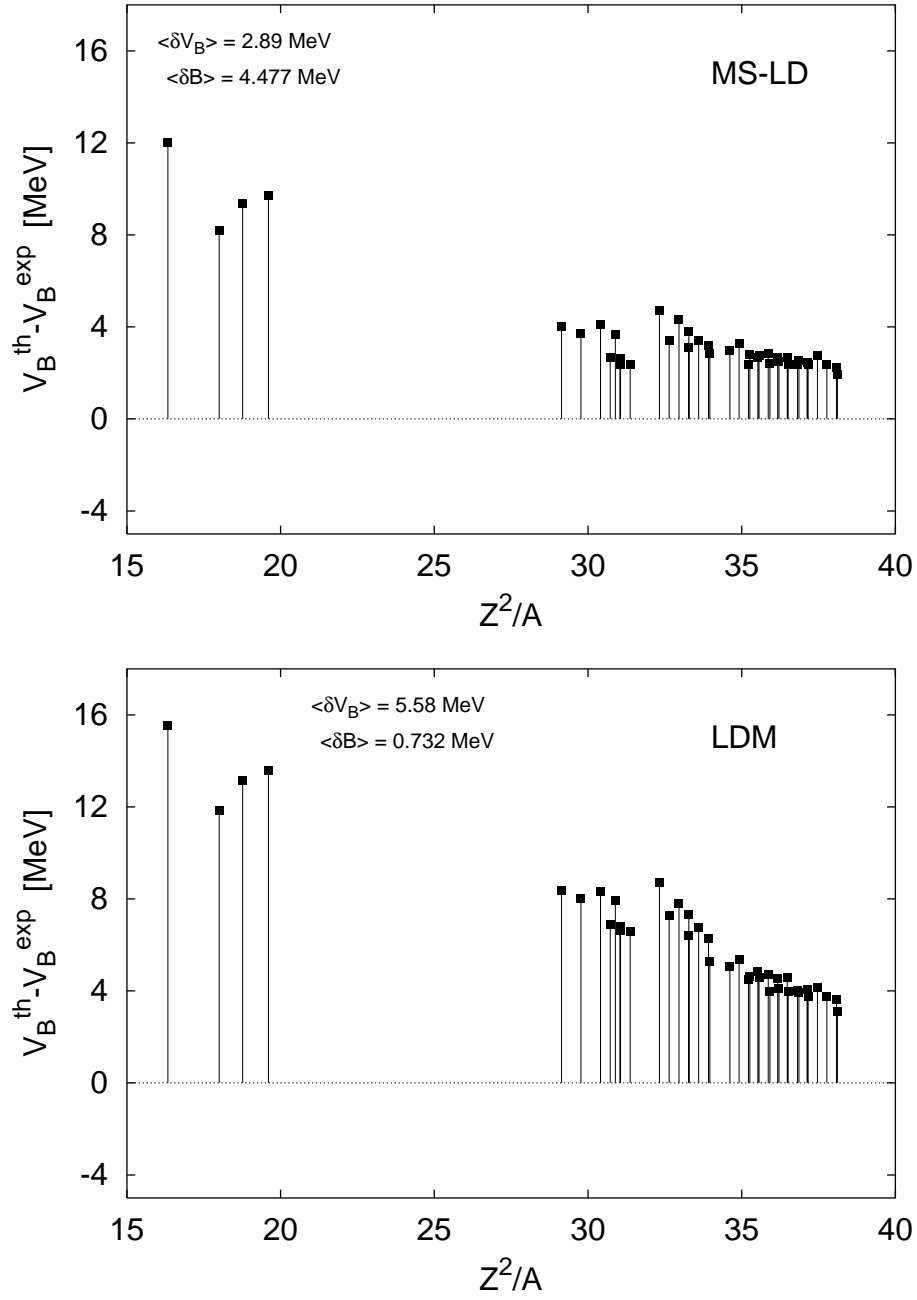


FIG. 4. The differences between the theoretical and experimental fission barriers heights obtained with the traditional Myers-Świątecki liquid drop (MS-LD) [26], top, and its modern version (LDM) obtained by the new fit to the *presently known* masses and microscopic corrections from Ref. [21], bottom. No information on the barrier heights has been used in the fitting procedure in this case.

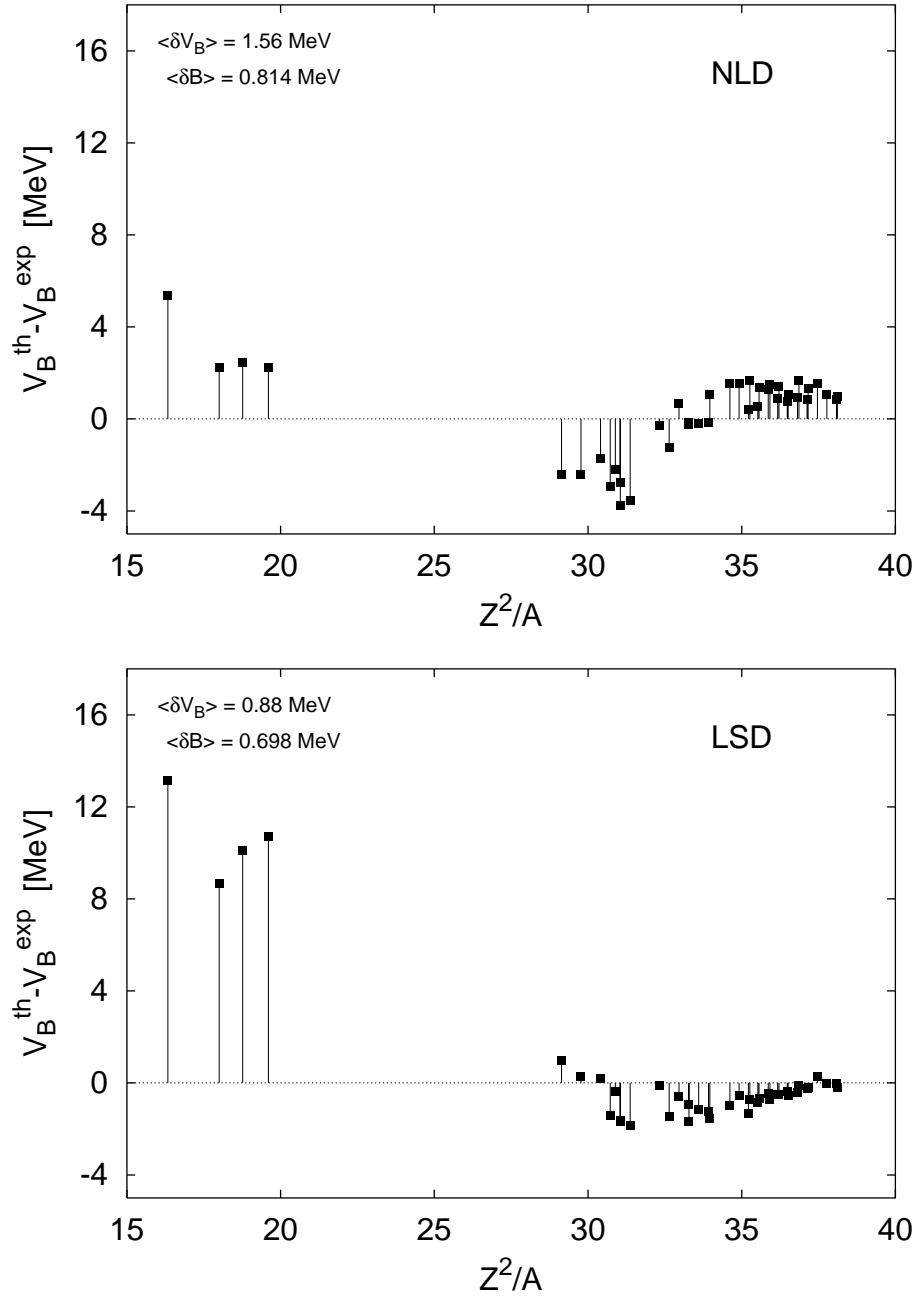


FIG. 5. Differences between the theoretical and experimental fission barrier heights obtained with a new liquid drop (NLD) model containing no first order curvature term (top) and with the Lublin-Strasbourg Drop (LSD) model which contains the first order curvature term (bottom). The LSD parameters were adjusted to the experimental binding energies only while the NLD ones were fitted to the measured fission barrier heights and to the masses.

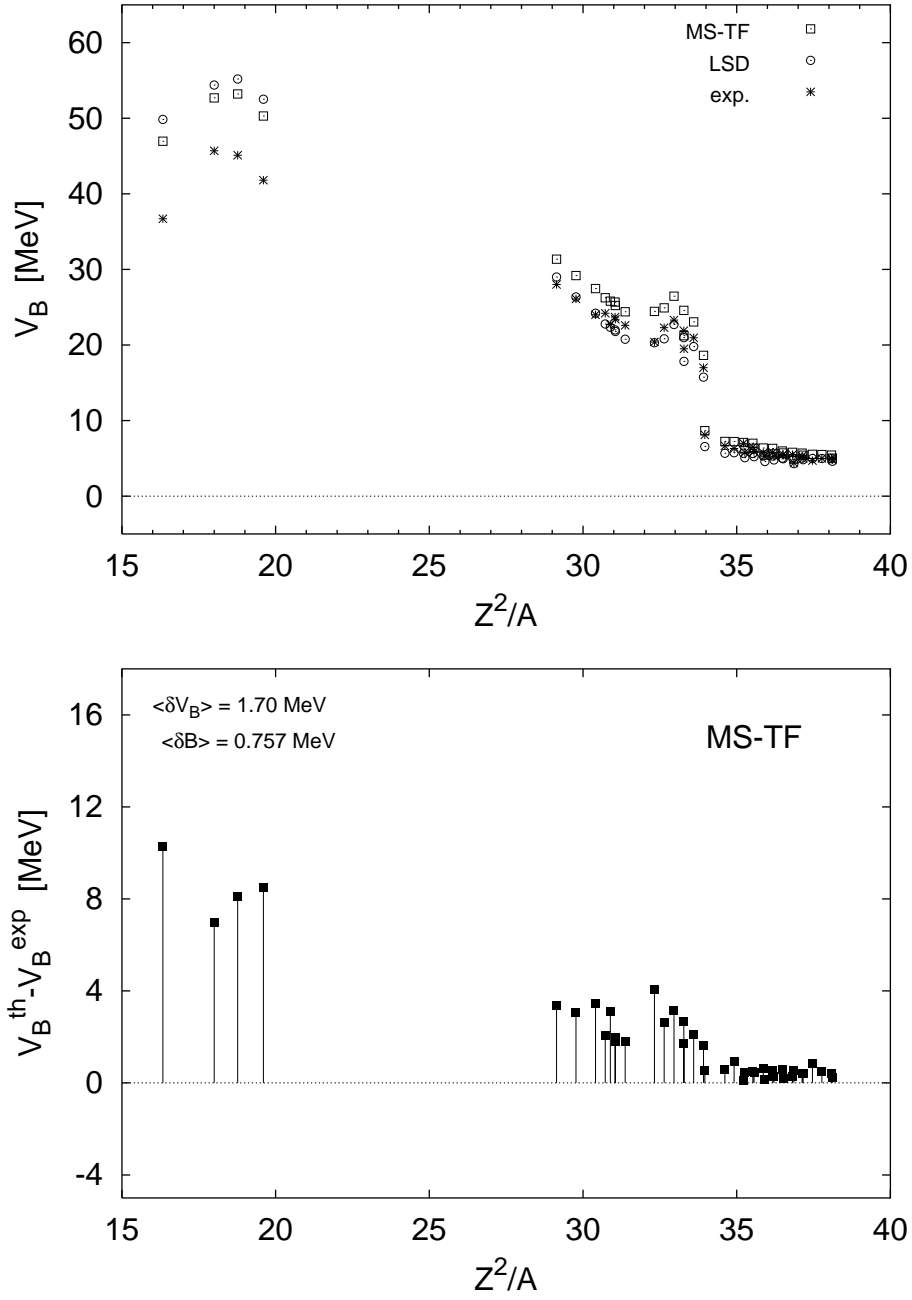


FIG. 6. Experimental fission barrier heights (see Refs. [18,22,33] and references cited therein), asterisks, compared to the theoretical ones obtained with the LSD (circles) and the Thomas-Fermi models of Ref. [18], open squares, (top). The differences between the Thomas-Fermi and experimental fission barrier heights are plotted in the bottom diagram.

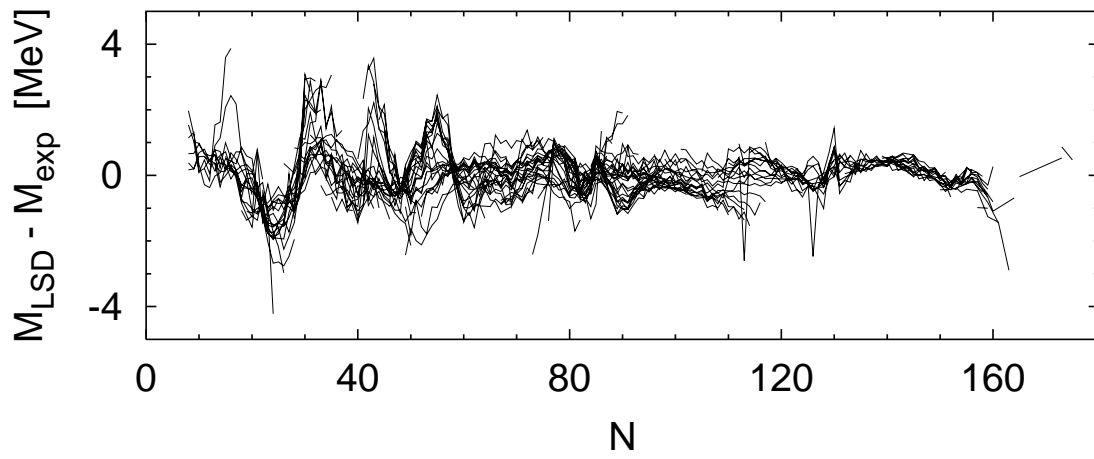


FIG. 7. Difference between calculated (LSD) and measured (exp.) masses for 2766 nuclei from the tables of Anthony. Lines connect the isotopes of each given element.



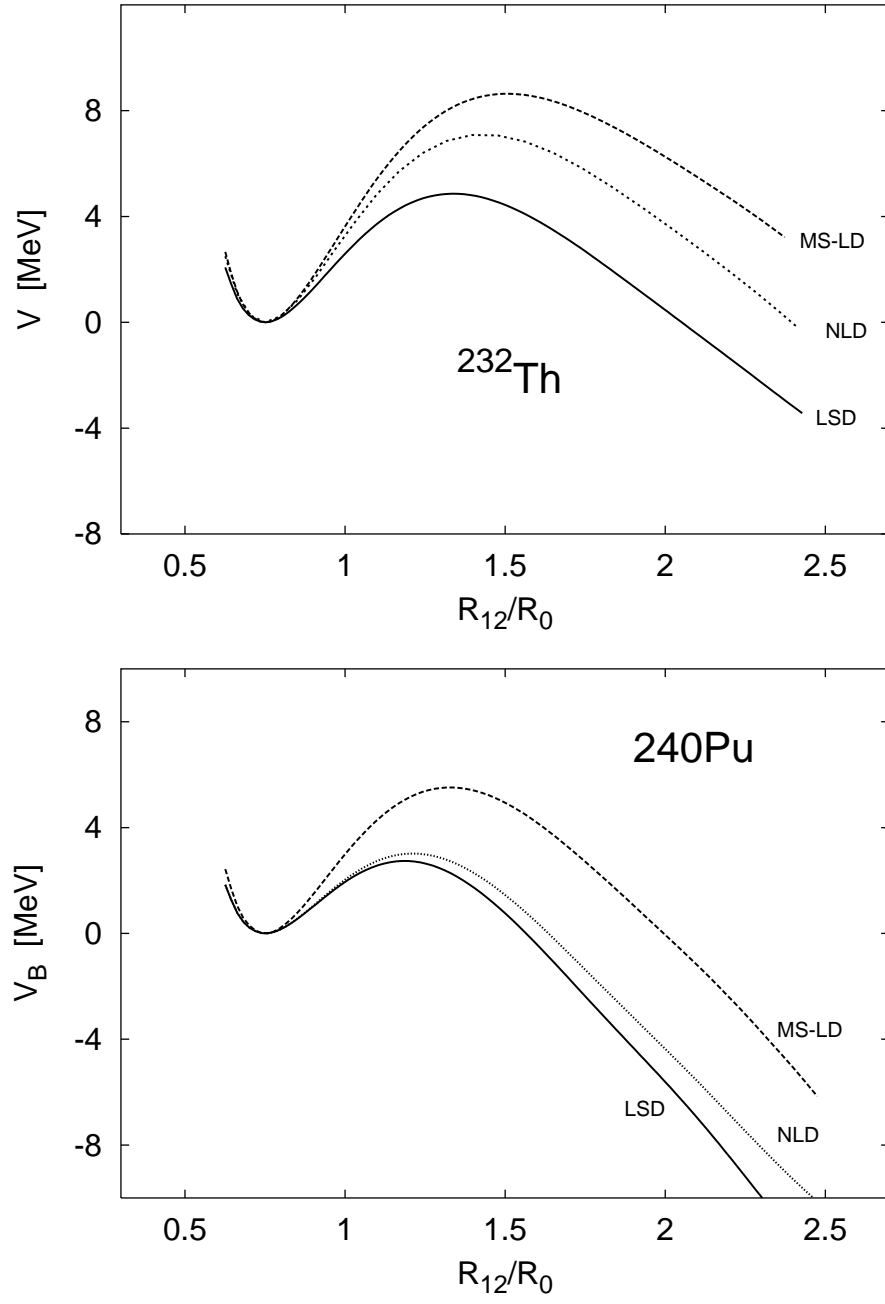


FIG. 8. Liquid drop fission barriers for  $^{232}\text{Th}$  (top) and  $^{240}\text{Pu}$  (bottom) obtained with the LSD, NLD and MS-LD sets of parameters.

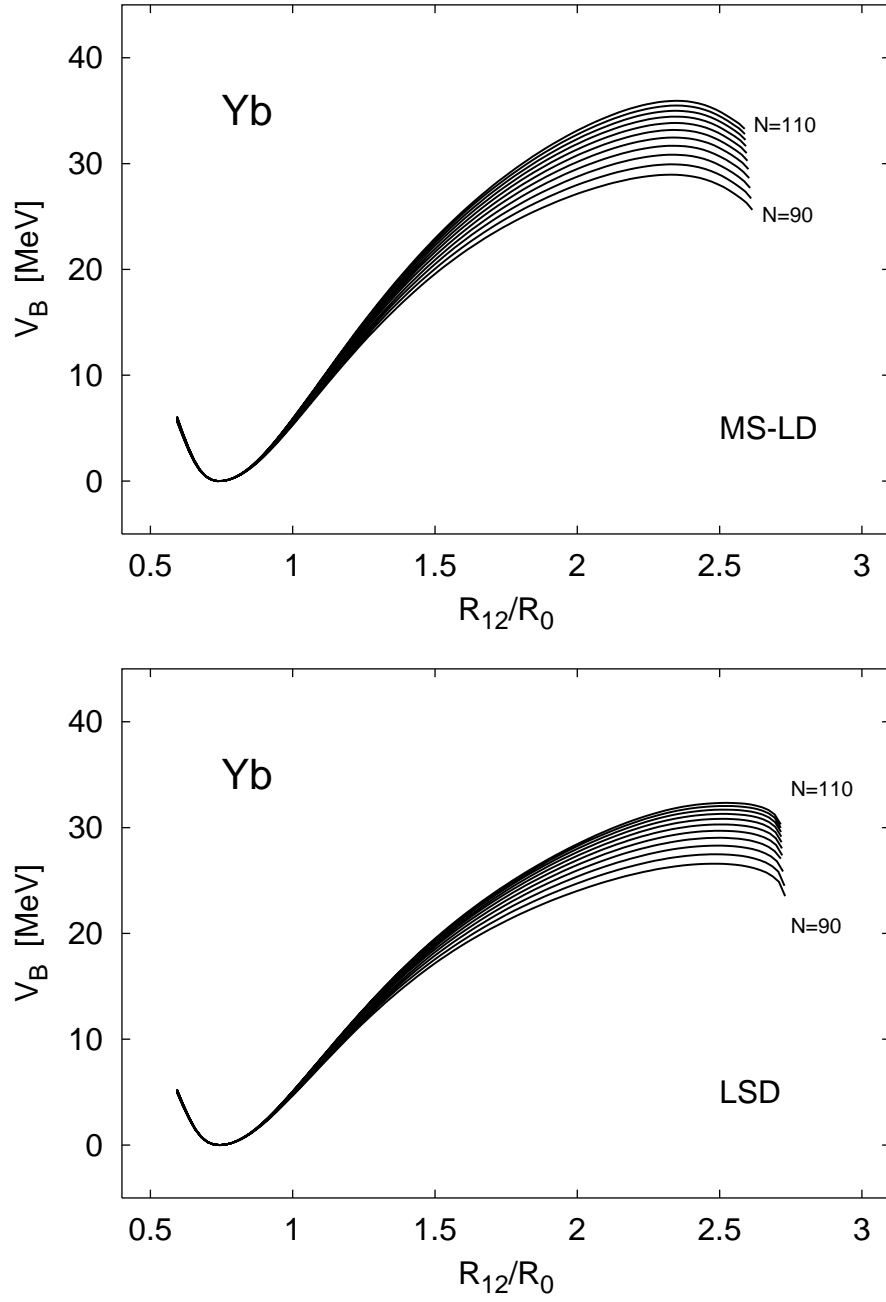


FIG. 9. Liquid drop fission barriers for Ytterbium nuclei according to the traditional (MS-LD) approach (top) and the curvature dependent formulation of the liquid drop model with the LSD parameterization (bottom). According to earlier predictions the Ytterbium range nuclei are likely to be sufficiently stable at the high spins to form the hyperdeformed configurations and the corresponding rotational bands.

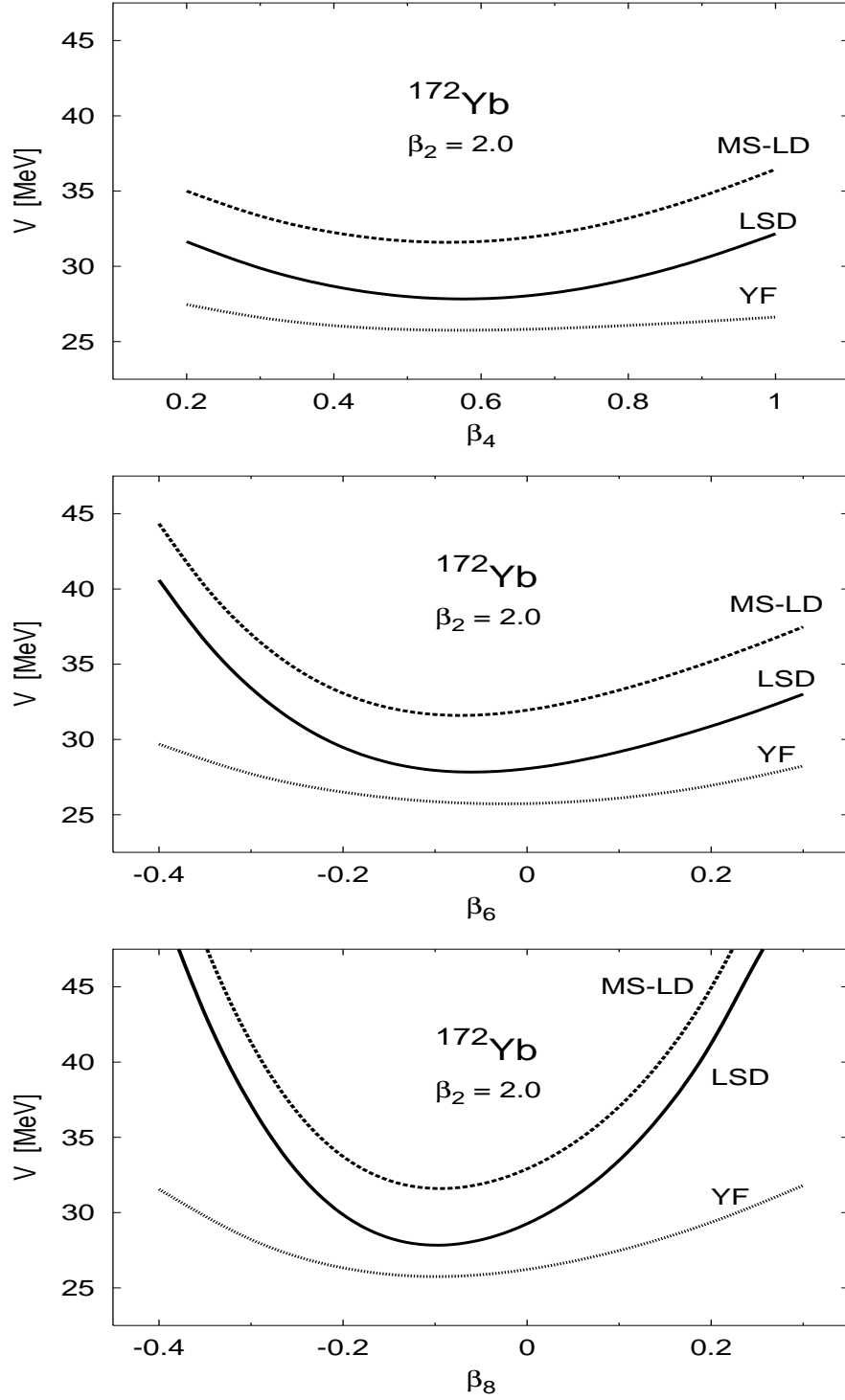


FIG. 10. Traditional (MS-LD) and curvature dependent (LSD) liquid drop energy of  $^{172}\text{Yb}$  around the saddle point ( $\beta_2=2.0$ ,  $\beta_4=0.582$ ,  $\beta_6=-0.058$ ,  $\beta_8=-0.108$ ,  $\beta_{10}=-0.001$ ,  $\beta_{12}=0.020$ ) as a function of the deformation  $\beta_4$  (top),  $\beta_6$  (middle) and  $\beta_8$  (bottom). For comparison the Yukawa-Folded (YF) macroscopic model results are shown.

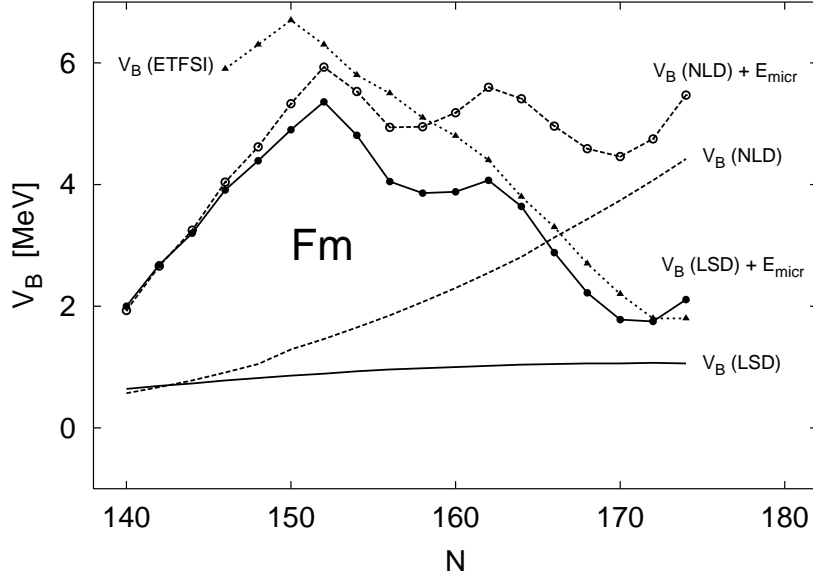


FIG. 11. Fission barrier heights ( $V_B$ ) of Fermium isotopes evaluated as the difference between the liquid-drop saddle-point energy and the ground state energy containing the microscopic corrections. The solid lines with the full dots correspond to the barriers calculated with the curvature dependent (LSD) model while the dashed lines with open circles represent the barriers calculated with the liquid drop model without curvature term (NLD). The difference between the full and the dotted lines is equal to the ground state microscopic correction taken from the tables [21]. The fission barriers obtained within the extended Thomas-Fermi model with the Skyrme interaction (ETFSI) [35] are drawn for comparison.

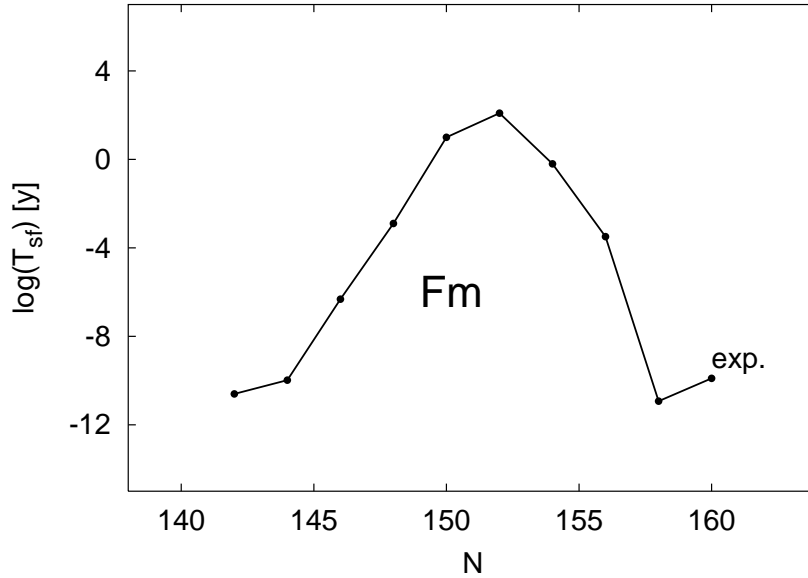


FIG. 12. Logarithm of the spontaneous fission life time [in years] of Fm isotopes. The full dots represent the experimental values. (cf. theoretical estimates in Fig. 11)